New effects in the multiphoton ionization of atoms

N. B. Delone and M. V. Fedorov

Institute of General Physics, Academy of Sciences of the USSR

Usp. Fiz. Nauk **158**, 215–253 (June 1989)

The review is devoted to new effects discovered recently in the course of studying the process of nonlinear ionization of atoms in the field of laser radiation—above-threshold ionization, manifestation of multielectron structure of complex atoms, formation of multiply charged ions, tunneling ionization, and emission of short-wavelength radiation. The main experimental data and their theoretical interpretation are presented. A discussion is given of the criteria for the applicability of the lowest non-vanishing order of non-steady-state perturbation theory to the description of the interaction of an atom with the electromagnetic field.

1. INTRODUCTION

Research into the nonlinear ionization of atoms, i.e. ionization caused by a time-varying electromagnetic field when the energy ω[1] of the radiation quantum is smaller than the electron binding energy $|\mathscr{E}_n|$ (where n is the principal quantum number of the state), began in the mid-1960's and proceeded apace to this day—probably reaching its widest scope at the present time. Hundreds of research papers, numerous reviews, and several monographs[1-12] have been devoted to the nonlinear ionization process. Nonetheless, there have only been a few, rather fragmentary efforts to generalize a number of new physical phenomena discovered in recent years. Thus a review of the latest research advances appears useful.

Research into nonlinear ionization of atoms can be divided into three periods. Although these periods do chronologically overlap to some extent, they are characterized by quite distinct conceptual frameworks.

The first period focused both theoretically and experimentally on the examination of the general features of the nonlinear ionization process. This period saw the development of a general theory of nonlinear ionization from a short-range potential, which made it clear that multiphoton ionization and the tunnel effect in a time-varying field are in fact two limiting cases of the same ionization process. Various researchers have observed multiphoton ionization of atoms and studied the main features of this process: the direct multiphoton ionization phenomenon (without intermediate resonances); the power law dependence $w^{(K)} \propto I^K$ of the direct ionization probability $w^{(K)}$ on the radiation intensity I, where K is the number of absorbed photons, which follows from conservation of energy, $K = \langle |E_0| w^{-1} + 1 \rangle |$ ($|E_0|$ is the ionization energy, $\langle ... \rangle$ indicates the integer part); the resonance ionization process, i.e. ionization involving an intermediate resonance between the energy of K' quanta ($K' < K$) and the energy of a bound electronic state in the atomic spectrum; the dynamical Stark effect and its contribution to resonances induced by an external field.

The second period was mainly concerned with the quantitative description of the direct and resonance varieties of multiphoton ionization of alkali atoms. Ionization was observed in relatively weak fields ($E < 5 \cdot 10^6$ V·cm^{-1} $= 10^{-3} E_a$, where $E_a = 5 \cdot 10^9$ V·cm^{-1} is the atomic field), such that the perturbation of the atomic spectrum by the radiation field was negligible.

In studying the direct process, the main experimental goal was to measure the multiphoton cross-sections $\alpha^{(K)}(\omega,\rho) = w^{(K)}/(I/\omega)^K$ as a function of frequency ω and polarization ρ of the radiation. The main theoretical problem was the calculation of these same $\alpha^{(K)}(\omega,\rho)$ cross-sections. In studying the resonance process, the main problem was the dependence of the resonance amplitude and lineshape in the ion yield on the various parameters characterizing the radiation field and the state participating in the intermediate resonance. The main conclusions obtained in the studies of multiphoton ionization of alkali atoms were the following: both the absolute magnitude of the direct (nonresonance) multiphoton ionization cross-section and its dependence on the frequency and polarization of the radiation field are adequately described by time-dependent perturbation theory in the first nonvanishing (K th) order; intermediate resonances (both single-photon and multiphoton) involve those atomic states into which transitions are allowed by the dipole approximation selection rules.

By the mid-1970's, the successful qualitative and quantitative description of the experimental data on multiphoton ionization of alkali atoms created the impression that even if some unsolved problems remained, they would be quantitative rather than qualitative in character. Perhaps the only fundamental problem unresolved by the late 1970's was the observation of nonlinear ionization in atoms where, according to the general theory, ionization should proceed by tunneling.

Precisely in that time period, however, a number of qualitatively new phenomena were observed. Interestingly, the discovery of these phenomena did not occur in the course of a coherent research effort, but rather randomly. Consequently, the first interpretations of some of these effects were altogether wrong. The new phenomena of greatest fundamental interest were the formation of doubly charged ions in the multiphoton ionization of alkaline-earth atoms[13] and the so-called above-threshold ionization of atoms.[14]

The very possibility of creating doubly charged alkaline-earth ions (Zapesochnyi and Suran[13] observed the formation of Sr^{2+} ions) in numbers comparable in order of magnitude to the yield of the singly charged species (see Fig. 1), in the multiphoton limiting case (the magnitude of the adiabaticity parameter being $\gamma \sim \omega/E \sim 10^2 \gg 1$), with the radiation field intensity much smaller than the atomic field ($E \sim 10^{-3}$), appeared at first glance to contradict completely the existing picture of the multiphoton ionization process. Indeed, since the first ionization energy of the strontium atom is $|\mathscr{E}_n^{(1)}(\mathrm{Sr})| \approx 5.7$ eV and the second ionization energy is $|\mathscr{E}_n^{(2)}(\mathrm{Sr})| \approx 11$ eV, at the laser photon energy of ≈ 1.2

 0038-5670/89/060500-21$01.80

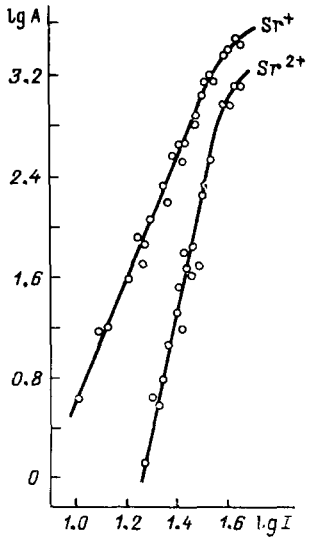

FIG. 1. The yield A of singly and doubly charged strontium ions as a function of laser intensity I.[13]

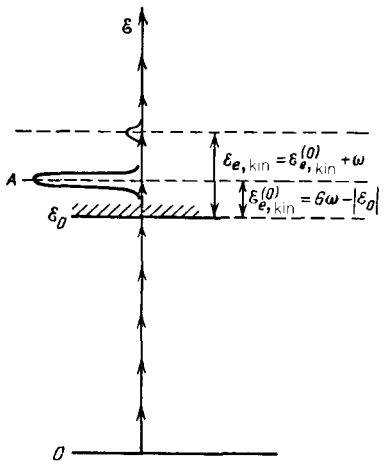

FIG. 2. Energy distribution $A(\mathcal{E})$ of electrons emitted in the 6-photon ionization of Xe.[14]

eV used for ionization in Ref. 13 the creation of a singly charged ion requires the absorption of five photons, whereas the creation of a doubly charged ion requires fifteen photons. Perturbation theory tells us that if the ionizing field is $E \ll 1$ we should expect $w^{(5)} \gg w^{(15)}$, and thus the approximately equal probability of forming Sr^+ and Sr^{2+}, given a fixed E and no saturation in the ion yield, appears to contradict sharply the general understanding of multiphoton ionization. Subsequently, multiply charged ions were observed in addition to the doubly charged species. In all cases, the probabilities of creating ions of different charge multiplicities did not differ appreciably at a fixed radiation field intensity.

The results of experiment[14] were equally surprising from the standpoint of the existing theory. That experiment focused on the energy spectrum of electrons emitted in the six-photon ionization of the xenon atom, carried out with $E \ll 1$ and $\gamma \gg 1$. In addition to the monoenergetic electrons with a kinetic energy $\mathscr{E}^{(0)}_{e,\mathrm{kin}} = 6\omega - |\mathscr{E}_0|$, expected from the conservation of energy in a six-photon ionization process, Agostini and co-workers[14] also observed monoenergetic electrons with energy $\mathscr{E}_{e,\mathrm{kin}} = \mathscr{E}^{(0)}_{e,\mathrm{kin}} + \omega$ (Fig. 2). At the same time, according to perturbation theory, in their experimental conditions the probability of absorbing seven photons should be vanishingly small compared to the probability of six-photon ionization. Later, electrons with energy $\mathscr{E}_{e,\mathrm{kin}} = \mathscr{E}^{(0)}_{e,\mathrm{kin}} + S\omega$ were observed. Depending on experimental conditions, the integer S would fall somewhere in the range between a few and several tens, and the ratio of probabilities of creating electrons in the main ($S = 0$) and additional ($S \geqslant 1$) peaks would also change.

Before proceeding with a discussion of these new phenomena, let us briefly turn to the advances in experimental techniques that have contributed greatly to the success of recent experiments.

The experimental details pertaining to the first and second periods of multiphoton ionization research have been exhaustively described in Refs. 2, 9, 10, 11. These experiments studied the ionization of ground state atoms using radiation in the visible and near infrared (IR) frequency ranges with laser pulses of nanosecond duration. With the field intensity $E \ll 1$, ionization was observed in the limiting multiphoton case, when $\gamma \gg 1$.

Advances in experimental techniques have improved practically all parameters of the studied atoms, the ionizing radiation, and the interaction process. Let us note some major advances. In addition to ground state atoms, recent experiments have studied the nonlinear ionization of Rydberg, i.e. highly excited atoms. Three new frequency ranges have become accessible: the ultraviolet ($\lambda < 100$ nm, $\omega > 10$ eV, infrared ($\lambda \sim 10$ μm, $\omega \sim 0.1$ eV), and UHF ($\lambda \sim 10$ cm, $\omega \sim 10^{-5}$ eV). Current experiments employ radiation fields of intensity $E < 1$ and $E \gtrsim 1$ (at the time of writing, the highest attainable intensity has reached 10^{17} $W \cdot cm^{-2}$). Ionization has been observed at $\gamma \ll 1$. Both picosecond (10^{-12} s) and femtosecond (10^{-15} s) laser pulses are currently available. Experiments now register the energy and angular distributions of electrons, as well as ions. Radiation from the interaction region also can be detected.

New methods and improved experimental conditions have made possible the observation of new phenomena in nonlinear ionization of atoms. In addition to the aforementioned above-threshold ionization and the formation of doubly charged alkaline-earth ions, new effects include the formation of multiply charged atomic ions, the tunnel effect in a time-varying field, ionization of Rydberg atoms by UHF radiation fields, as well as a large number of phenomena associated with the formation of singly charged ions that cannot be interpreted in the single-electron approximation. Below we shall briefly examine the more important new phenomena, with the exception of the ionization of Rydberg atoms in UHF fields. The latter is a qualitatively different process which is best treated by classical mechanics rather than quantum mechanics.[15-17]

2. ABOVE-THRESHOLD IONIZATION OF ATOMS

2.1. Main features of the process

Experimentally, the studies of above-threshold ionization focus on the energy and angular distributions of the

emitted electrons. In interpreting the electronic spectra, one must take into account the spatial and temporal nonuniformity of the ionizing laser field. This factor enters into all experiments on laser-induced atomic ionization. The duration of the laser pulse τ_l typically lies in the 10^{-7}–10^{-13} s range, with the laser light focused onto a spot $\Phi \sim 10$–100 μm in extent. The spatial and temporal nonuniformity gives rise to two effects. First, the observed phenomena represent a sum of the effects of different fields on different atoms. Second, both the energy and the angular distributions of the electrons can generally change on the way to the detector due to ponderomotive forces[18] arising in a spatially nonuniform field of focused laser radiation. These ponderomotive forces have no effect on the energy and emission angle of the electron as long as the electron does not move appreciably from its origin during the interaction time with the radiation field. In the above-threshold ionization process, electron energies fall into the 1–10 eV range and hence the electron velocities are of the order of 10^8 cm·s^{-1}. Consequently, the electron can move up to 10 μm in a time t_0 of the order of 10^{-11} s. In order to suppress the effects of ponderomotive forces one requires ultrashort laser pulses of duration $\tau_l < t_0$. Yet the vast majority of the experiments employ long (on this time scale) laser pulses $\tau_l > t_0$, which makes it difficult to discern the properties of the elementary process.

We also note that although the conditions of all experiments precluded particle collisions in the focused beam spot over the duration of the laser pulse, it is still possible that the interaction of differently charged particles played a role in some experiments. Charged particle interaction can broaden the energy peaks and distort the angular distribution of electrons. Estimates performed in Ref. 19 indicate that this interaction can be neglected only if the density of charged particles is less than 10^{10} cm^{-}3.

Let us now turn to a brief phenomenological description of above-threshold ionization. Later we shall try to distinguish the properties of the elementary ionization of a single atom from the effects arising due to ponderomotive forces.

In the vast majority of experiments which observed above-threshold ionization, the radiation intensity was in the 10^{12}–10^{14} W·cm^{-2} range. As a rule the first above-threshold peaks in the energy spectrum appear at the lower limit of this range, $I_{th} \sim 10^{12}$ W·cm^{-2}. As the radiation intensity is increased above I_{th}, the number of peaks quickly increases. The typical evolution of the electron energy spectrum is shown in Fig. 3 (data from Ref. 20). Clearly, beginning with some critical intensity I_{cr}, the amplitudes of some higher order peaks begin to exceed the preceding peaks. A significant number of lower order peaks can be suppressed in this manner.[21]

The above-threshold ionization process is characterized by yet another radiation intensity I_{sat}. When $I > I_{sat}$, the ionization process saturates ($w\tau_l > 1$, where w is the ionization probability per unit time). In this case, all atoms in the focused beam spot are ionized during the laser pulse and hence the ion yield ceases to depend on I.

When $I < I_{sat}$ and the pulse duration is not ultrashort, the total number of ions and electrons created during the laser pulse is proportional to I^K, where K is the minimal number of absorbed photons required for ionization.[20] This general dependence follows from the first nonvanishing

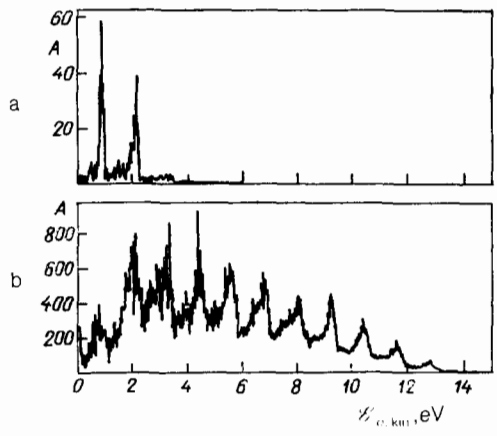

FIG. 3. Distribution of electrons emitted in the 11-photon ionization of Xe as a function of electron kinetic energy $\mathcal{E}_{e,kin}$.[20] A is the signal amplitude at the electron detector in rel. units that are the same for distributions a and b: (a)—radiation intensity $I = 1$ (rel. units); (b)—$I = 2$.

(Kth) order of perturbation theory and is typical for the limiting multiphoton case of nonlinear ionization. At first sight, above-threshold ionization appears to contradict this well-known result. Yet this process can be explained by assuming that deviations from perturbation theory in the partial probabilities $w^{(K+S)}$ occur at lower radiation field intensities than the total probability

$$w = \sum_S w^{(K+S)}.$$

Calculations performed in Ref. 22 support this conclusion. When the pulse duration is ultrashort ($\tau_l \sim 2 \cdot 10^{-14}$ s) the data deviate from the $w \propto I^K$ law.[23] We note that I_{sat} is larger in the case of ultrashort laser pulses.

The particular values of I_{th}, I_{cr}, and I_{sat} depend on the type of atom and radiation frequency employed in the experiment. There are indications that I_{cr} is larger for the hydrogen atom than for more complex atoms, all other conditions being equal.[24,25] However, in all experiments the three characteristic intensities I_{th}, I_{cr}, and I_{sat} correspond to the limiting multiphoton case, which is characterized by the adiabaticity parameter $\gamma \sim \omega/E \gg 1$. Consequently, the phenomenon of above-threshold ionization is unrelated to the tunnel effect in a time-varying field.

A typical difference in the angular distribution of electrons that are emitted in different above-threshold S peaks in the energy distribution is shown in Fig. 4.[26] Figure 5 illustrates a perturbation theory calculation for the hydrogen atom,[28] which is in good agreement with experimental data.[27] The general tendency is for the angular distribution to become less isotropic as the number S of absorbed above-threshold photons increases—the electrons are emitted mainly parallel and antiparallel to the electric field vector.

The above-threshold ionization process also depends on the polarization of the radiation. In the case of circular polarization, the amplitude of above-threshold peaks is much reduced (all other experimental conditions being equal) and these peaks are shifted towards higher values of S. Qualitatively this behavior is due to the higher values of orbital angular momentum in the final state and the large repulsive centrifugal potential[29] that arises when the field is circularly polarized.

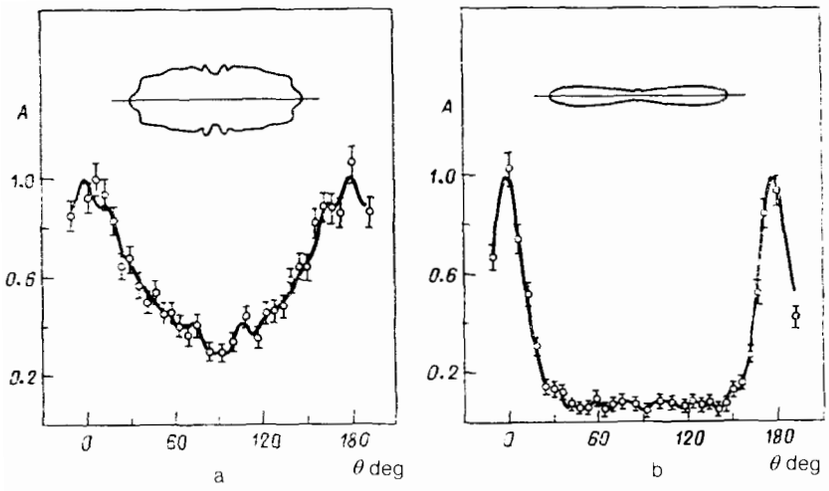

FIG. 4. Angular distributions of emitted electrons in the 11-photon ionization of Xe.[26] a—Data for the first peak in the electron energy distribution. b—Data for the peak corresponding to the above-threshold absorption of four photons ($S = 4$). A is the signal amplitude at the electron detector in rel. units that are the same for distributions a and b. Error bars indicate the statistical confidence in the values of the signal A. The emission angle is measured to better than 10°.

Finally, we shall mention one other experimental fact: when long radiation pulses (in the above sense, $\tau_1 > t_0$) are employed, the positions of the above-threshold peaks in the electron energy distribution becomes independent of the radiation intensity; whereas in the case of short radiation pulses ($\tau_1 < t_0$) there is a shift towards lower energies proportional to the radiation intensity.[20,30,31]

Looking ahead, we note that although a great many researchers have studied the above-threshold ionization effect, we are far from a quantitative explanation of all the experimental facts. Such an explanation would come in three parts: a description of the elementary ionization process, including the effects of nonmonochromatic radiation and of the noninstantaneous switching on and off of the interaction; treatment of the spatial nonuniformity of the field; and an account of the influence of ponderomotive forces on the energy and angular distributions of detected electrons. In the following sections we shall separate these three components of the above-threshold ionization process and distinguish the features which are already understood from those that require further elaboration.

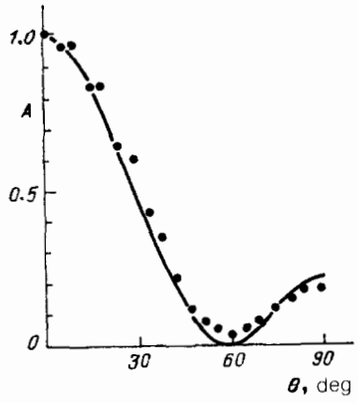

FIG. 5. Angular distribution of emitted electrons in the four-photon ionization of the hydrogen atom by radiation with $\lambda = 355$ nm. Points are experimental[27]; the solid curve is theoretically calculated.[28] A is the signal amplitude at the electron detector in rel. units.

2.2. Perturbation theory

We have already noted that the detection of electrons with kinetic energy

$$\mathcal{E}_{e,\ kin} = \mathcal{E}_{e,\ kin}^{(0)} + S\omega$$

in the limiting multiphoton case of nonlinear ionization ($\gamma \gg 1$) in fields $E \ll 1$ essentially appears to contradict perturbation theory estimates. A detailed treatment of this apparent contradiction is evidently the key issue in the perturbation theory description of the interaction between a strong electromagnetic field and an atomic system.

The problem consists of computing correctly the K th and $(K+1)$st order component matrix elements. The magnitude of the critical intensity I_{cr} can be obtained from the condition that the ratio of these matrix elements is unity. These matrix elements have been computed both numerically[25,28,32] and analytically in the semiclassical approximation.[33,37,38]

Regions of the discrete and continuum spectra close to the ionization threshold (in the continuum this is the region $\mathcal{E} \ll 1$) can be treated semiclassically. In these regions the complicated expressions of the Coulomb matrix elements[35,36] are greatly simplified.[33,34] Thus, for example, the matrix element of the $\mathbf{d}\cdot\mathbf{E}_0/2$ operator (where d is the dipole moment) between two continuum states with energies $\mathcal{E}$, $\mathcal{E}' \ll 1$ can be written as[37]

$$V_{\mathcal{E}\mathcal{E}'} = \frac{1}{2}(\mathbf{d}\mathbf{E}_0)_{\mathcal{E}\mathcal{E}'} \sim \frac{E_0}{|\mathcal{E}' - \mathcal{E}|^{5/3}} = \frac{E_0}{\omega^{5/3}} \qquad (1)$$

where the continuum wavefunctions are normalized to a δ-function of the energy difference between $\mathcal{E}$ and $\mathcal{E}'$, and the last equality is obtained by setting $|\mathcal{E}' - \mathcal{E}| = \omega$.

The $(K+1)$st order matrix element $M_{\mathcal{E}_0}^{(K+1)}$, which describes the transition of the electron from the ground state (0) to the final state of energy

$$\mathcal{E} = \mathcal{E}_0 + (K+1)\omega$$

(for the first above-threshold maximum $S = 1$), contains K sums and integrals over the intermediate bound and continuum states. We can separate the component of $M_{\mathcal{E}_0}^{(K+1)}$ which corresponds to the multiphoton "resonance" with the continuum states of energy $\mathcal{E}_0 + K\omega$ (where $\mathcal{E}_0$ is the ground state energy), and write $M_{\mathcal{E}_0}^{(K+1)}$ in the form

$$M_{\mathscr{E}0}^{(K+1)} = -\int d\mathscr{E}' \frac{M_{\mathscr{E}'0}^{(K)} V_{\mathscr{E}\mathscr{E}'}}{\mathscr{E}' - (\mathscr{E} - \omega) + i0} + (M_{\mathscr{E}0}^{(K+1)})_{nr} \tag{2}$$

where $(M_{\mathscr{E}0}^{(K+1)})_{nr}$ is the part of the matrix element that sums over the nonresonant discrete intermediate states with energies $\mathscr{E} = \mathscr{E}_0 + (K+1)\omega$. The first term on the right of equation (2) can be rewritten as the sum of a principal value integral and an integral over a δ-function. The δ-function integral gives

$$(M_{\mathscr{E}0}^{(K+1)})_{tot} = i\pi M_{\mathscr{E}-\omega,0}^{(K)} V_{\mathscr{E},\mathscr{E}-\omega}. \tag{3}$$

Following Ref. 38 we assume that the contribution to $(M_{\mathscr{E}0}^{(K+1)})_{tot}$ of both the principal value integral and the $(M_{\mathscr{E}0}^{(K+1)})_{nr}$ term of equation (2) is small compared to the δ-function integral (3). The approximation in which the full matrix element is replaced by (3) is known as the factored matrix element approximation or the pole approximation. In this approximation we find, from equation (1), that the amplitude ratio of the first above-threshold peak to the main peak is of the order of magnitude

$$V^2 = \frac{E_0^2}{\omega^{10/3}}. \tag{4}$$

This result explains qualitatively why above-threshold ionization does exist and why fields much smaller than the atomic field can still cause sizeable deviations from perturbation theory. According to (4) the reason is that the frequency ω is small compared to the atomic frequency $\omega_a \sim 10^{16}\ s^{-1}$ (in the atomic system of units $\omega \ll 1$). Consequently the matrix elements for transitions to the continuum are anomalously large, which leads to sizeable deviations from perturbation theory results and to the appearance of pronounced above-threshold peaks at radiation intensities

$$I \sim I_{cr} \sim \omega^{10/3} \ll 1. \tag{5}$$

Generally speaking, the underlying assumption that the principal value integral contribution to $M_{\mathscr{E}0}^{(K+1)}$ (as well as the $(M_{\mathscr{E}0}^{(K+1)})_{nr}$ contribution) is small compared to the pole term (3) is not rigorously justified. There exists no smallness parameter that justifies the neglect of these terms. However, there are indications that the neglected terms in the matrix elements are small because the contribution from the region where $\mathscr{E}'$ is very close to $\mathscr{E}$ (satisfying the inequality $|\mathscr{E}' - \mathscr{E}| < \mathscr{E}^{3/2} \ll \mathscr{E} \ll 1$) compensates for the region of $\mathscr{E}'$ far from $\mathscr{E}$ ($|\mathscr{E}' - \mathscr{E}| > \mathscr{E}^{3/2}$).[39,40] To sum up, currently the estimates of I_{cr} from expression (5) can be taken as valid only within an order of magnitude.

Taking into account the neglected terms in (2) can quantitatively alter these estimates, but probably would not change the qualitative dependence of V^2 (4) and I_{cr} (5) on ω.

Now let us discuss the connection between the expressions we derived for V^2 and I_{cr} and the dynamical Stark effect. We know[2] that the Stark shift of the energy level $\mathscr{E}_n$ in a time-varying field is $-(1/4)\alpha_n(\omega)E_0^2$, where $\alpha_n(\omega)$ is the dynamic polarizability which approximately equals $-\omega^2$ as long as $\mathscr{E}_n < \omega \ll 1$. The shift of the higher-lying (Rydberg) levels and of the atomic ionization threshold equals the oscillation energy of a free electron in the time-varying electric field $\delta\mathscr{E} = E^2/4\omega^2$. The shift in the binding energy of the ground state is

$$\delta\mathscr{E}_0 = \frac{1}{4} E_0^2 (\omega^{-2} - \alpha_0(\omega)). \tag{6}$$

In noble gas atoms $\alpha_n(\omega) \sim \alpha_n(0) \sim 1$ for helium and ~ 27 for xenon. Therefore, when $\omega < 10^{-1}$, the following relations hold

$$|\alpha_0(\omega)| \ll \omega^{-2}, \quad \delta\mathscr{E}_0 \sim \delta\mathscr{E} = E_0^2/4\omega^2.$$

If $\delta\mathscr{E} > \omega$ the first above-threshold peak can fall below the ionization threshold and hence disappear. Consequently, the condition $\delta\mathscr{E} \sim \omega$ determines the characteristic parameter $V'^2 = E_0^2/\omega^3$, which limits the region of applicability of perturbatin theory, and the corresponding critical intensity $I'_{cr} \sim \omega^3$. Since we have $\omega \ll 1$, the parameter V'^2 is smaller than V^2, and I'_{cr} is larger than I_{cr} (5). Consequently, it is the semiclassical nature of the Coulomb transitions near the threshold, rather than the dynamical Stark effect, that limits the region of applicability of perturbation theory and determines the critical intensity. We emphasize that this effect essentially arises from the Coulomb interaction between the emitted electron and the remaining ion, because the Coulomb interaction determines the form of quasiclassical matrix elements (1).

In the case of a short-range potential, the matrix element (1) is replaced by the expression

$$V_{\mathscr{E}\mathscr{E}'} \sim E_0 \mathscr{E}^{1/2} \operatorname{Re} \frac{1}{(\mathscr{E}' - \mathscr{E} + i0)^2}, \tag{7}$$

which is valid for the entire quasiclassical region $\mathscr{E}, \mathscr{E}' \ll 1$, regardless of the energy separation between $\mathscr{E}$ and $\mathscr{E}'$. In the case of a Coulomb potential, formulae (1) and (7) are valid in the regions $|\mathscr{E}' - \mathscr{E}| > \mathscr{E}^{3/2}$ and $|\mathscr{E}' - \mathscr{E}| < \mathscr{E}^{3/2}$ respectively.[39,40] When $|\mathscr{E}' - \mathscr{E}| = \omega$ and $\mathscr{E} \sim \omega$, formula (7) yields $V_{\mathscr{E}\mathscr{E}'} \sim E_0/\omega^{3/2}$ and hence V^2 (see (4)) is replaced by V'^2 and I_{cr} (see (5)) by I'_{cr}. In the case of the short-range potential, the parameter which characterizes the applicability of the first nonvanishing order of perturbation theory and the critical radiation intensity coincide with the parameters imposed by the dynamical Stark effect. Note, that even though I'_{cr} is larger than I_{cr} of (5), I'_{cr} is still $\ll 1$ as long as $\omega \ll 1$. Consequently, even though the critical intensity is larger in a short-range potential than in a Coulomb potential, it is still much smaller than the atomic intensity. We know that the short-range potential model to a first approximation describes negatively charged ions. Hence, according to the above arguments, we should expect to observe above-threshold photoionization in negatively charged ions at intensities $I > I'_{cr} > I_{cr}$. Currently no experimental data are available in this regard.

Let us also consider the numerical calculations for the hydrogen atom[25] carried out within perturbation theory. The results of these calculations indicate that the true frequency dependences of $w^{(K)}(\omega)$ and $w^{(K+1)}(\omega)/w^{(K)}(\omega)$ are considerably more complex than the qualitative semiclassical results. The probability $w^{(K+1)}(\omega)$ has resonances at discrete levels (Fig. 6). The ratio $w^{(K+1)}(\omega)/w^{(K)}(\omega)$ also has minima and maxima (Fig. 7): the minima correspond to resonance peaks in the frequency dependence $w^{(K+1)}(\omega)$, whereas the maxima correspond to the valleys between resonances. The peak to valley ratios in the $w^{(K+1)}(\omega)/w^{(K)}(\omega)$ function are numerically estimated

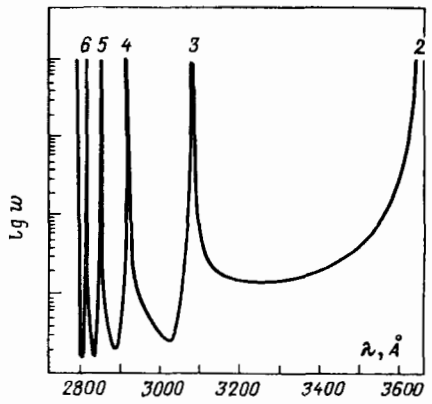

FIG. 6. Ionization probability of the five-photon above-threshold ionization of the hydrogen atom (rel. units) as a function of radiation wavelength λ at $K = 4$. The numbers label the principal quantum numbers of the discrete levels which contribute intermediate resonances. The curve was calculated using perturbation theory.[25]

as ~ 2. Table I cites the value of $w^{(K+1)}/w^{(K)}$ at four arbitrary points. There is a clear general tendency for this ratio to increase as λ increases (or ω decreases). We note that the calculated values of $w^{(K+1)}/w^{(K)}$ in Ref. 25 are in good agreement with experimental data[24] obtained at $\lambda = 3076$ Å.

Table I indicates that the calculated values are $I_{cr} \sim 10^{14}$ W·cm^{-2} at $\lambda \sim 500$ nm and $\sim 10^{13}$ W·cm^{-2} at $\lambda \sim 10^3$ nm. These values are significantly larger than the experimentally measured I_{cr} in noble gas atoms[41] ($\sim 10^{12}$ W·cm^{-2} and $\sim 10^{11}$ W·cm^{-2}). Accordingly, I_{cr} must depend strongly on the type of atomic species under study, and particularly on the magnitude of the ionization potential (at a given ω). Yet this behavior is not reflected in expression (5) and, to our knowledge, no simple qualitative theoretical explanation exists to date.

In Fig. 7 the ratio $w^{(K+1)}/w^{(K)}$ is plotted against $\lambda^{10/3} \propto \omega^{-10/3}$, which simplifies comparison with the semiclassical approximation, where the result would be a straight

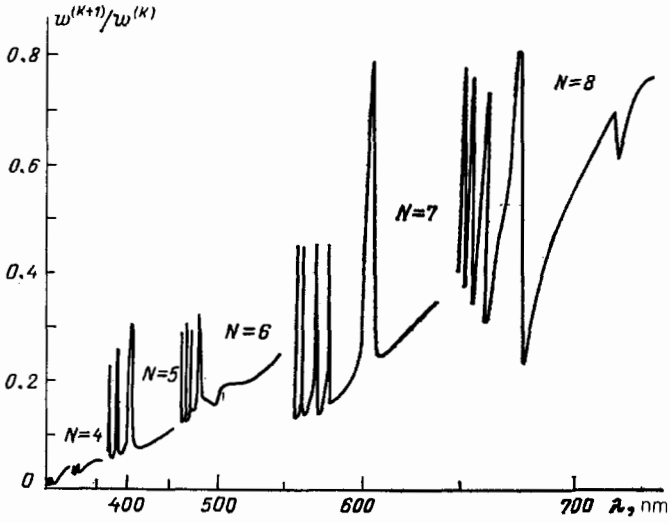

FIG. 7. Probability ratios of $K + 1$ and K-photon ionizations of the hydrogen atom as functions of $\lambda^{10/3}$. The curve was numerically calculated using perturbation theory.[25]

line. At first glance it would appear that the numerical calculations do not fit the semiclassical result. Yet recall that the peak to valley ratio of the $w^{(K+1)}/w^{(K)}$ curve is small and the semiclassical formulae yield the values of V^2 (see (4)) and I_{cr} (see (5)) up to a factor of two. Thus the numerical calculations do coincide with semiclassical results within their actual accuracy.

To sum up, the main success of the semiclassical results lies in their explanation of the apparent contradiction between the observation of above-threshold ionization and perturbation theory arguments. They indicate why deviations from perturbation theory occur even when the external field is much weaker than the atomic field, the reason being that the matrix elements for transitions to the continuum are large at $\omega \ll 1$.

2.3. Models of strong interaction in the continuum

These models treat the multiple electronic transitions between continuum states (in the continuous spectral range) under the influence of an external time-varying field. In essence, this class of models comprises the classic papers of 1960's—1970's on nonlinear ionization of atoms,[42–46] together with qualitatively similar recent studies.[47,48] However, one should be cautious in applying these results to the above-threshold ionization process. The point is that, first, all the above studies assumed the atomic potential to be short-range, i.e. they neglected the effect of the real atomic Coulomb potential on the continuum electron wavefunctions. Second, the final results in Refs. 42–44, 47, 48 are obtained by way of various simplifying assumptions which are not rigorously justified. To wit, the results of different studies yield different symbolic parameters which determine the required ratio of ionization probabilities calculated in the K + 1st and K th orders of perturbation theory. Thus, according to Refs. 42, 44, when $\gamma \gg 1$ this ratio is

$$\frac{w^{(K+1)}}{w^{(K)}} \sim \frac{1}{\gamma^2} \sim \frac{E^2}{\omega^2},$$

whereas Refs. 43, 45–47 find a different ratio

$$\frac{w^{(K+1)}}{w^{(K)}} \sim \frac{E^2}{K^2\omega^3} \sim \frac{E^2}{\omega}.$$

Moreover, both these parameters are quite different from the semiclassical estimate for the short-range potential

$$\frac{w^{(K+1)}}{w^{(K)}} \sim \frac{E^2}{\omega^3}.$$

Accordingly, the semiclassical critical radiation intensity I'_{cr} for above-threshold ionization is much smaller than the results of Refs. 42–47. We believe this semiclassical estimate to be more reliable, since it was obtained within the framework of perturbation theory without any additional assumptions.

The last few years have witnessed much research on the strong interaction models. We shall discuss the more complete model of Deng and Eberly.[49] Generally, the Schrödinger equation is used to derive and solve the system of coupled equations for the probability amplitudes of finding the atom in the ground state and the various continuum states, where the equations include the Coulomb interaction between the electron and the atom.

The particular version of this approach, realized by Deng and Eberly[49] made use of the "significant state meth-

TABLE I. Calculated ratios of the probability $w^{(K+1)}$ of creating an electron in the first above-threshold peak to the probability $w^{(K)}$ of creating one in the threshold peak as a function of wavelength λ in the ionization of a hydrogen atom.[25]

	$K=2$	3	7	8
λ, Å	1216	2432	6155	7181
$w^{(K+1)}/w^{(K)}$ $(10^{15}\ \mathrm{W\cdot cm^{-2}}/I)^{-1}$	0,1	2	25	70

od." One of the main approximations of Ref. 49 is the so-called "pole approximation" which is essentially similar to the factorization of matrix elements (3) described in the previous section. Keeping in mind the arguments made earlier about the validity of expression (3), we can assume by analogy that the model of Ref. 49 yields only a qualitatively correct explanation of the elementary above-threshold ionization process. Going beyond the pole approximation can quantitatively alter the results of Ref. 49, whose main conclusions can be summarized as follows:

1) a saturation parameter Z is introduced, which is essentially identical to the quantity V^2 determined by expression (4); the condition $Z\sim 1$ fixes the value of I_{cr} and the estimates for this critical intensity coincide with the semiclassical result (5);

2) the first few peaks in the energy distribution will become partially saturated in the $I_{cr}<I<I_{sat}$ intensity range; the height of each peak is proportional to $I^{K-(1/2)}$, i.e. increases more slowly with I in this range than if $I<I_{cr}$; the width of the peaks is of the order of τ_1^{-1} (the field is assumed to be monochromatic); the number of the peaks is $S\sim V$;

3) in the $I>I_{sat}$ intensity range the first few peaks are strongly broadened and suppressed; the number of the peaks remains $S\sim V$, their height is proportional to $I^{K-(1/2)}$ and their width to I^K;

4) when $I<I_{sat}$ the probabilities $w^{(K+S)}$ of above-threshold ionization increase linearly with pulse duration τ_1; when $I>I_{sat}$ the probabilities $w^{(K+S)}$ are independent of τ_1.

Thus the new results which go beyond perturbation theory apply to the $I>I_{sat}$ intensity range.

Note the fourth conclusion of Ref. 49. The described dependence $w^{(K+S)}\sim\tau_1$ clearly indicates that above-threshold ionization is neither a cascade nor a diffusive process. By a cascade process we mean the sequential overpopulation of the continuum states: $\mathscr{E}_0\to\mathscr{E}_0+K\omega\to\mathscr{E}_0+(K+1)\omega\to\mathscr{E}_0+(K+2)\omega$ and so forth. A diffusive process refers to the case when the state $\mathscr{E}_0+(K+S)\omega$ undergoes transitions to "higher" and "lower" states (i.e. to $\mathscr{E}_0+(K+S+1)\omega$ and $\mathscr{E}_0+(K+S-1)\omega$, respectively) with approximately equal probability, leading to diffusive broadening of the probability envelope.[50] Both these possibilities are excluded because the require different dependences $w^{(K+S)}\times(\tau_1)$ that would disagree with the results of Ref. 49. Movsesyan and Fedorov[51] discovered the reason for the saturation of $w^{(K+S)}$ (τ_1) at sufficiently large τ_1. They pointed out that the ionization process coherently populates the continuum states (creating wavepackets). Subsequent transitions between these states interfere with one another. As a consequence one obtains $w^{(K+S)}$ $(\tau_1)=$ const as soon as τ_1 becomes greater than the inverse width of the wavepacket $(\Delta\mathscr{E})^{-1}$.[49] In the case of above-threshold ionization, this width $\Delta\mathscr{E}$ coincides with the ionization broadening of the main level and the condition $\tau_1>(\Delta\mathscr{E})^{-1}$ is the saturation criterion (full ionization of the atoms).

The authors of Ref. 49 considered a one-dimensional model of the atom, ignoring the orbital angular momentum degeneracy of the continuum states. This factor was treated properly in Ref. 52. It follows from these studies that taking into account orbital angular momentum degeneracy does not alter the qualitative predictions of Ref. 49 about the nature of the above-threshold ionization. On the other hand, the totality of states with different orbital angular momenta must be considered in order to treat the angular distribution of photoelectrons. The theoretical predictions in Ref. 52 are in qualitative agreement with experimental data[26,27,53]: the lower-lying above-threshold peaks are created by a superposition of states with not-too-large orbital angular momentum L; as the photoelectron energies (and the numbers of the above-threshold peak S) increase, so does the contribution of spherical harmonics and intermediate values of L to the excited states.

We note that a number of studies[54–56] examined alternative models of strong interaction in the continuum, which in some sense contradict the model of Ref. 49. The difference between these models is easily demonstrated in the weak field limit. The alternative models[54–56] proposed that the main contribution to the $M_{\mathscr{E}_0}^{(K+1)}$ matrix element arises from the principal value of the integral, rather than the δ-function. The principal value of the integral is largely determined by the region of $\mathscr{E}'$ close to $\mathscr{E}$. Mathematically the formal result is to replace $V_{\mathscr{E}\mathscr{E}'}$ by $\delta(\mathscr{E}'-\mathscr{E})$ (with $V=pA$, where A is the vector potential of the field). However, as we have discussed above, a careful analysis of the $V_{\mathscr{E}\mathscr{E}'}$ matrix element shows that the contribution of the region where $\mathscr{E}'$ is fairly close to $\mathscr{E}$ is small and hence the principal value of the integral is also small. Consequently we belive these alternative models[54–56] to have little physical content. In choosing between the approaches of Ref. 49 and Refs. 54–56 we believe Ref. 49 to be more reliable, once the above factors are taken into account.

A serious flaw of all strong interaction models[49,52,54–56] is the assumption that the interaction is switched on instanly, together with their neglect of the shifts in the energy levels and the ionization threshold due to the dynamical Stark effect. Consequently the results of Ref. 49 apply only to a limited range of intensities $I<I'_{cr}\sim\omega^3$ (see above, section 2.2). Since the intensity range from I_{cr} (determined by expression (5)) to I'_{cr} is rather narrow, it is not clear whether it is possible to compare in detail those predictions of the strong interaction models[49,52] which differ from per-

turbation theory results with any experimental data.

In view of these limitations, the strong interaction models[49,52,54-56] cannot describe the suppression of lower-lying above-threshold peaks by the increasing ionization threshold when $I > I'_{cr} \sim \omega^3$. In this regard, let us mention an *ab initio* numerical solution of the one-dimensional Schrödinger equation with the $-(1+X)^{-1/2}$ potential in the field of an electromagnetic wave.[57] This approach to the $I > I'_{cr}$ intensity range does predict the "closing" of above-threshold ionization channels due to the increase in the ionization threshold by the quantity $E_0^2/4\omega^2$.

Before proceeding to the available experimental data on the elementary ionization process and to the comparison of this data with the theory, let us discuss the ponderomotive potential and its effect on the energy and angular distributions of electrons traveling from the ionization region to the detector. Only after elucidating the role of the ponderomotive potential can one discern the effects characteristic of the elementary process.

2.4. The role of the ponderomotive potential

As we have mentioned earlier, the distribution of the laser radiation over the ionization region is markedly nonuniform. The nonuniformity of the spatial distribution leads to the appearance of ponderomotive forces,[15] which arise from the gradient of the ponderomotive potential. The notion of the ponderomotive potential in a spatially nonuniform field is conveniently introduced by averaging the Hamiltonian of a nonrelativistic electron in a time-varying field $E = E_0(r)\sin\omega t$ over the rapid oscillations with frequencies ω and 2ω[58]:

$$H = \frac{1}{2}\overline{\left(p + \frac{E_0(r)}{\omega}\sin\omega t\right)^2} = \frac{p^2}{2} + \frac{E_0^2(r)}{4\omega^2}. \qquad (8)$$

The second term on the right hand side of expression (8) describes the potential energy arising from the ponderomotive potential. The corresponding ponderomotive force $-\nabla E_0^2(r)/4\omega^2$ is known in the literature as the gradient force (or, occasionally, the Gaponov–Miller force[59]).

The influence of the ponderomotive potential on the electron energy consists of the following: if an atom is ionized at point r_0 then the potential energy of the emitted electron decreases by $E_0^2(r_0)/4\omega^2$ as it leaves the focal beam spot and the kinetic energy increases by the same quantity.

Obviously the effect of the ponderomotive potential increases at low radiation field frequencies. This is experimentally observed by electron spectroscopy in the ionization of noble gas atoms by the infrared field of a CO_2 laser.[60]

At the typical frequency $\omega \sim 1$ eV employed to investigate the above-threshold ionization of atoms, an electron leaving the focal beam spot gains from 0.1 eV kinetic energy at $I \sim 10^{12}$ W·cm^{-2} to 10 eV at $I \sim 10^{14}$ W·cm^{-2}. In order for the electron to leave the focal spot during the laser pulse, the pulse duration must be sufficiently long. The appropriate estimates were performed in section 2.1. They show that only picosecond and femtosecond laser pulses are short enough to keep the electron from escaping the focal beam spot. Thence it follows, at first glance, that in the vast majority of the experiments performed with long laser pulses, the ponderomotive acceleration of electrons should significantly distort the positions of the above-threshold peaks on the energy scale of the elementary ionization process. In fact no such distortion occurs because of the dynamical Stark effect.

As noted above, the shift in the ionization threshold in noble gas atoms due to the dynamical Stark effect is practically equivalent to the mean electron oscillation energy in the electromagnetic field, that is $E_0^2/4\omega^2$. Hence, the shift in the ionization threshold due to the dynamical Stark effect reduces the kinetic energy of the continuum electron to compensate almost precisely the kinetic energy gained by the electron as it is accelerated by the ponderomotive potential. For this reason, the electron spectra obtained in the above-threshold ionization of noble gases are not distorted by the ponderomotive acceleration and should reflect the elementary ionization process. Note that this compensation is only valid for noble gas atoms and for wavelengths that are not too short (near ultraviolet, visible, and infrared), such that the dynamic polarizability of the ground state can be neglected in comparison with the vibrational energy of a free electron in the time-varying field. For most other atoms this is not the case, as is already evident from well-known measurements of static polarizability.[61]

In the general case, the kinetic energy of electrons outside the focal spot is described by the equation

$$\mathscr{E}_{e,km}^{(S)} = (K+S)\,\omega + \mathscr{E}_0 + \frac{E_0^2(r_0)}{4\omega^2} - \frac{E_0^2(r_0)}{4}(\omega^{-2} - \alpha_0(\omega)) \approx \mathscr{E}_0 + (K-S)\,\omega \qquad (9)$$

where the approximate equality is obtained by assuming $\alpha_0(\omega) \ll \omega^{-2}$.

Many authors have reported that the electron energy does not depend on the radiation intensity in experiments measuring the above-threshold ionization of noble gases, for example in Refs. 21, 53, 62. An explanation of this effect similar to the one cited above was first furnished in Refs. 63, 64.

The ponderomotive acceleration can also broaden the above-threshold peaks. This broadening is caused by the nonstatic nature of the electromagnetic field, i.e. its time dependence $E_0 = E_0(r,t)$. If the ponderomotive potential changes during the time it takes for the electron to leave the focal spot, the Stark shift compensation will be insufficient (or excessive) and the electron energy will differ from $\mathscr{E}_{e,km}^{(S)}$ given by expression (9). It is a simple matter to estimate the corresponding change in $\mathscr{E}_{e,km}^{(S)}$:

$$\Delta\mathscr{E} \sim \Delta t \frac{\partial}{\partial t}\frac{E_0^2(r,t)}{4\omega^2} \sim \frac{\Delta t}{\tau_{cl}}\frac{E_0^2}{4\omega^2}. \qquad (10)$$

Since the photoelectrons are created at different moments in time, $\partial E_0/\partial t$ can have arbitrary magnitude and sign, and the energy shifts will be different for different electrons. This contributes to peak broadening, the scale of which is set by expression (10). The broadening of above-threshold peaks caused by the time-dependence of the ponderomotive potential explains the experimental data[53] shown in Fig. 8.

The ponderomotive potential can also markedly alter the angular distribution of the electrons. In a uniform field the photoelectrons mostly propagate parallel or antiparallel to the field polarization vector. Ponderomotive acceleration acts in the opposite direction to the potential gradient. If the focal spot is more or less symmetric in all directions, the ponderomotive acceleration of emitted electrons will smooth out their angular distribution, making it more iso-

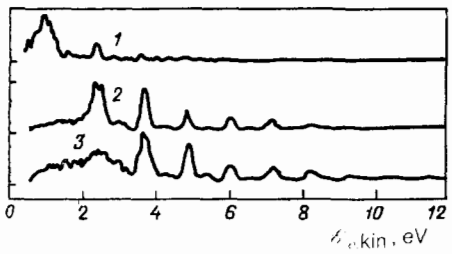

FIG. 8. Experimental data illustrating the broadening of peaks in the energy spectrum as the intensity increases[53]: 1—$I = 5.6 \cdot 10^{13}$; 2—$I = 10.2 \cdot 10^{13}$; 3—$I = 14.1 \cdot 10^{13}$ W·cm^{-2}.

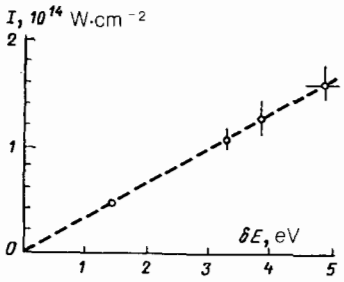

FIG. 9. Experimental data illustrating the role of the dynamical Stark effect in above-threshold ionization[31]: δE is the energy shift of a given above-threshold peak, I is the field intensity.

tropic. Furthermore, this smoothing effect will be strongest in the lower above-threshold peaks. As for the higher-lying above-threshold peaks, there the initial kinetic energy of the electrons is large and both the kinetic energy gain and trajectory bending are relatively small—hence the weaker smoothing effect. These qualitative arguments agree well with the data of Ref. 53.

We emphasize that this explanation is an alternative to the analyses[28,52] which explain the angular distribution of above-threshold electrons by the properties of the elementary ionization process. Both these approaches lead to qualitatively similar conclusions which agree with experiment.[26,27,53] At this time it is difficult to establish which effect determines the directionality of the emitted above-threshold electrons—their acceleration by the ponderomotive potential or the specifics of the ionization process.

2.5. Above-threshold ionization caused by short laser pulses

If the pulse duration is smaller than the time of flight of the electron escaping from the focal spot, the electron cannot be accelerated by the ponderomotive potential. After the pulse is switched off, the electron ionized at point r_0 in the focal spot remains with the kinetic energy

$$\mathcal{E}_{e\,kin}^{(S)} = \mathcal{E}_0 - (K - S)\,\omega - \frac{E_0^2(r_0)}{4}(\omega^{-2} - \alpha_0(\omega))$$

$$\approx \mathcal{E}_0 - (K - S)\,\omega - \frac{E_0^2(r_0)}{4\omega^2}. \qquad (11)$$

This kinetic energy depends on the intensity of the radiation at the point where ionization takes place. As the intensity increases, the electron kinetic energy decreases, which is corroborated by experiment.[30,31,65]

Muller and co-workers[31] measured the shift in the above-threshold peaks of xenon atoms ionized by 100 fs pulses at $\lambda = 670$ nm. They found these shifts to be linear in intensity, with the maximum shift energy reaching 5.6 eV. By that point the first two above-threshold peaks fell below the ionization threshold and the corresponding photoelectrons were not detected. This brings up one of the previously discussed mechanisms for the experimentally observed suppression of the first few above-threshold peaks: if the Stark shift of the ionization threshold exceeds ω (or, equivalently, $E_0 > \omega^{3/2}$), the electrons cannot reach the continuum and these peaks can no longer be observed.

This explanation applies to both short and long pulses, since the Stark shift of the ionization threshold is independent of the influence of the ponderomotive potential on the electrons traveling from the atom to the detector. However, this interpretation presupposes the absence of saturation, which is significant. The saturation intensity for this experiment was $I_{sat} = 1.7 \cdot 10^{14}$ W·cm^{-2}.[31] Only in the absence of saturation ($I_{max} < I_{sat}$) does most of the ionization occur at the center of the focal spot where $I = I_{max}$, leading to a significant Stark shift of the ionization threshold ($E_0 > \omega^{3/2}$).

The experimental conditions of Ref. 30—$\tau_l = 500$ fs, $\lambda = 616$ nm—appear very similar to those of Ref. 31. And yet the results of these two experiments are different in many respects. The authors of Ref. 30 observed a saturation intensity $I_{sat} = 3.1 \cdot 10^{13}$ W·cm^{-2}. Possibly this pronounced difference from the result of Ref. 31 is explained by the five-fold increase in the pulse duration. Unlike Ref. 31, the experiment[30] exhibited several clear instances of resonance ionization (see below), which possibly enhanced the ionization efficiency and decreased I_{sat}.

The resulting spectrum of above-threshold electrons is markedly affected by the ratio between the peak laser pulse intensity I_{max} and the saturation intensity I_{sat}. The shift of the above-threshold peaks was observed both at $I_{max} < I_{sat}$[31] and $I_{max} > I_{sat}$,[30] but as saturation is reached and $I_{max} > I_{sat}$[30] the shift of the peaks also saturates (Fig. 10). The last two curves in Fig. 10, corresponding to different pulse durations and intensities I, almost coincide. This saturation and the high degree of nonlinearity make it possible to construct a model of nearly step-like ionization. If the maximum intensity in the focal spot is $I_{max} > I_{sat}$, the ionization occurs mostly at those points in the focal spot and at those moments in time when $I(r,t) \approx I_{sat}$. The following interpolation formula for the probability of K-photon ionization per unit time at the point r was employed for numerical modeling[30]:

$$w^{(K)}(r, t) = \Gamma_i(r, t) \exp\left(-\int_{-\infty}^{t} \Gamma_i(r, t')\,dt'\right). \qquad (12)$$

where $\Gamma_i(r,t) \propto (I(r,t)/I_{sat})^K$ is the ionization broadening of the main level; $I(r,t)$ is the laser field intensity at the point r at time t. The total probability is calculated by integrating $w(r, t)$ over its arguments. This calculation yielded the curves in Fig. 10 which were in good agreement with experimental results.[30] Evidently, when saturation occurs at $I_{max} > I_{sat}$, the previously discussed mechanism of the suppression of the first few above-threshold peaks by the large Stark shift of the ionization threshold may no longer apply. That mechanism applies only if the Stark shift is larger than ω at $I = I_{sat}$. Otherwise the peaks shift by less than ω, remain

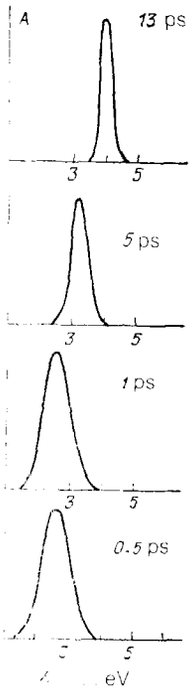

FIG. 10. Experimental data[30] illustrating the saturation of the energy shift of the above-threshold peaks that follows the saturation of the ionization process. A is the signal amplitude at the electron detector in rel. units that are the same for all curves.

above the ionization threshold, and cannot be suppressed in this way. The evolution of the above-threshold peaks as a function of I_{max}, I_{sat}, and τ_1 at $I_{max} > I_{sat}$ has not been studied in detail.

In addition to the aforesaid shift of the above-threshold peaks, an important advance achieved by going to short laser pulses was the discovery of fine structure in the above-threshold ionization spectrum. Figure 9 shows the fine structure of the first above-threshold peak in the 7-photon ionization of Xe by $\lambda = 616$ nm radiation with intensity $I = 3.9 \cdot 10^{14}$ W·cm^{-2} and pulse duration $\tau_1 = 0.4$ ps. The physical interpretation of the observed fine structure runs as follows. In a strong field all the highly-excited atomic levels gain a Stark shift energy of $E_0^2/4\omega^2$, which is equal to the vibrational energy of a free electron in a time-varying field. Furthermore, if the ionization process is nonresonant in a low field, at high fields the large Stark shift can move relatively low-lying atomic levels up to energies near resonance (for example, up to $\mathscr{E}_0 + (K-1)\omega$). This enhances the ionization probability. The condition for the Stark shift to move some level of energy $\mathscr{E}_i < \omega$ into resonance with $(K-1)$-photon absorption can be written as

$$\mathscr{E}_0 + (K-1)\,\omega = \mathscr{E}_i + \frac{E_0^2(r,\,t)}{4\omega^2}. \qquad (13)$$

Equation (13) will determine the values of r and t that would satisfy the appropriate resonance conditions for a given energy level $\mathscr{E}_i$. Since the pulse duration τ_1 is assumed to be short, the kinetic energy of electrons in some above-threshold peak S is determined by equation (11). Taking (13) into account for the $(K-1)$-photon resonance via the Stark-shifted level we obtain

$$\mathscr{E}_{e,\,sat}^{(S)} = \mathscr{E}_0 + (K+S)\,\omega - \frac{E_0^2(r,\,t)}{4\omega^2} = \mathscr{E}_i + (S+1)\,\omega. \qquad (14)$$

Thus, each resonance level $\mathscr{E}_i$ should produce a resonance peak in the fine structure of above-threshold ionization. In Fig. 11 these peaks are identified by comparison with reference data on the Xe atom. The good agreement with experimental data for a large number of peaks led Freeman and co-workers[30] to conclude that up to the 7p and 4f atomic levels in Xe the Stark energy shift agrees with the vibrational energy of a free electron to fairly high precision.

The appearance of fine structure in above-threshold peaks caused by resonances with discrete levels shifted by $E_0^2/4\omega^2$ was theoretically predicted in Ref. 66, whose authors solved the Schrödinger equation with the $-1/(1-x^2)^{1/2}$ potential.

2.6. Conclusion

The current understanding of above-threshold ionization can be summarized in the following fashion. There is much interesting experimental data available. Qualitative explanations exist for most of these experimental results. Also, a number of models have been developed to describe the elementary process of above-threshold ionization, but the quantitative predictions of these models are not entirely satisfactory because of the insufficiently justified approximations involved.

Several key features of above-threshold ionization remain unexplained. Not even a qualitative explanation exists for the fact that in the $I_{cr} < I < I_{max}$ intensity range the total flux is $\propto I^K$ and yet the probability $w^{(K+S)}$ is not proportional to I^{K+S}. The semiclassical results (4) and (5) await sufficiently detailed experimental corroboration. We still cannot predict the characteristic values of I_{sat}. Some uncertainties remain in our understanding of the evolution of above-threshold peaks produced by short pulses of intensity $I_{max} > I_{sat}$.

The extension of semiclassical arguments to the energy range near the ionization threshold has been an important theoretical advance. The semiclassical results explain the anomalously large values of continuum-continuum transi-

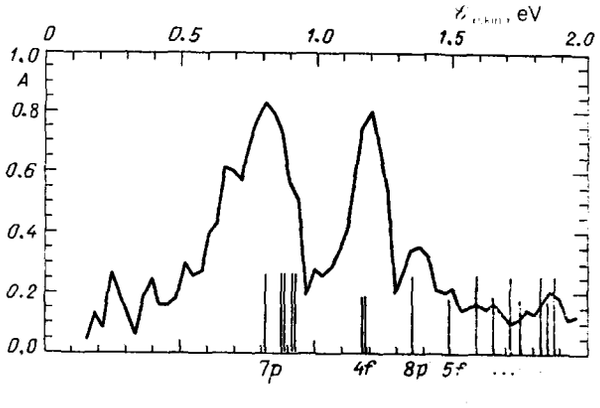

FIG. 11. Experimental data[30] illustrating how the intermediate multiphoton resonances in the atomic spectrum (resonance states are indicated) manifest themselves in the electron energy spectrum in above-threshold ionization. A is the signal amplitude at the electron detector in rel. units.

tion matrix elements (1) and the correspondingly low critical intensity I_{cr} (5) above which the energy structure of the above-threshold photoelectron spectrum becomes discernible. The second important theoretical contribution has been the numerical solution of the hydrogen atom problem and the detailed examination of various calculated quantities.[25] The third and final important advance has been the detailed development and application of the concept of the ponderomotive potential.[24,30,63,64]

As for the above-threshold ionization phenomena, we believe the observation of fine structure in the above-threshold ionization spectra[30] to hold much interest and promise in the field of nonlinear laser spectroscopy. Another very recent discovery that should bolster the importance of above-threshold ionization has been the experimentally established connection between this process and the multiple ionization of atoms. This series of questions, including the role of above-threshold ionization, will be discussed in section 4 of this review.

3. MANIFESTATIONS OF THE MULTIELECTRON STRUCTURE OF COMPLEX ATOMS IN SINGLE-ELECTRON MULTIPHOTON IONIZATION

It is well known that the electronic state spectrum differs markedly among different types of atoms—the hydrogen atom, atoms with one electron in the outer shell (alkali elements), and atoms with many equivalent outer shell electrons. In addition to singlet states, the latter also possess triplets, coupled multielectron states, and autoionizing states with energies near the first ionization potential. Undoubtedly the very existence of these states can influence the multiphoton ionization process. Manifestations of multielectron structure can appear in the absolute magnitude of multiphoton cross-sections, in the angular distributions of emitted electrons, and in the spectrum of intermediate resonance frequencies. From the theoretical point of view, the presence of multielectron states requires one to abandon the single-electron approximation in describing the multiphoton ionization of complex atoms. A detailed theoretical description of the multiphoton ionization of atoms in the single-electron approximation already exists[2,3,7,10] and furnishes good agreement with experimental data on alkali atoms. The question arises as to whether the single-electron approximation remains valid for the ionization of atoms with many electrons in the outer shell.

Let us consider the various aspects of single-electron multiphoton ionization of atoms with many electrons in the outer shell that may shed light on those effects that are not explained by the single-electron approximation.

3.1. Absolute magnitudes of multiphoton cross-sections for the direct (nonresonance) ionization process

There have been numerous measurements of the absolute magnitudes of multiphoton cross sections for the direct ionization of atoms with many electrons in the outer shell—alkaline-earth atoms (see, for example, Ref. 67) and noble gas atoms.[68] The main conclusion of these experiments was that these cross sections coincide within experimental accuracy with their alkali atom counterparts.[10,11] Consequently, in such integral characteristics of the ionization process as the multiphoton cross sections, the presence of many electrons does not significantly alter the quantities whose order of magnitude can be estimated in the single-electron approximation.

3.2. Probability of the direct single-electron multiphoton ionization process as a function of radiation polarization

In the case of direct (nonresonance) multiphoton ionization of alkali atoms, circular polarization is more effective than linear polarization when the process is only slightly nonlinear.[2,3,10,11] At a fixed frequency, the ratio of ionization probabilities is

$$\frac{w_{\mathrm{circ}}^{(K)}}{w_{\mathrm{lin}}^{(K)}}=\frac{(2K-1)!!}{K!}, \tag{15}$$

where K is the nonlinearity order of the ionization process. Strictly speaking this ratio is not valid for all frequencies. The exceptions include the narrow frequency ranges in each nonresonance interval where $w_{circ}=0$ and those resonance frequencies where the selection rules allow resonance with linearly polarized light but not with circularly polarized light. The ratio (15) is theoretically justified if the transition channel from the ground state to the continuum in the linearly polarized field satisfies Bethe's rule (the largest matrix elements correspond to transitions with $n\to n+1$, $L\to L+1$, where n and L are the principal and orbital quantum numbers respectively)[69] and also K is not too large. The upper bound on K follows from the approximation that only transition channels where L increases are taken into account in a linearly polarized field, while the other channels are neglected. Kraĭnov and Melikishvili[70] demonstrated that in this approximation the ratio (15) is valid for transitions from the ground state with an arbitrary L and does not depend on the type of binding prevalent in the complex atom. Consequently, as long as the single-electron approximation holds, this ratio should apply to the ionization of alkaline-earth atoms.

The dependence of the single-electron multiphoton ionization probability on polarization, as well as the validity of ratio (15), were experimentally investigated in the alkaline-earth atoms by many researchers. It was established that in nearly all studied systems the ratio (15) does not hold. In some cases the ratio was even reversed and the ionization probability in a linearly polarized field dominated. This problem was exhaustively investigated in Ref. 71. The authors measured the three-photon ionization of Ba, Sr, and Ca atoms by laser radiation in the 19700–23100 cm^{-1} frequency range. The working frequencies were selected such that the component matrix elements corresponding to direct multiphoton ionization were dominated by the transition channel satisfying Bethe's rule. They measured the ratios of ionization probabilities in linearly and circularly polarized fields in wide frequency bands near 12 intermediate two-photon resonances with singlet states: from 4s5d to 4s7d; from 5s6d to 5s11d; and from 6s9d to 6s12d. In all cases the experimental ratio w_{circ}/w_{lin} was much smaller than the value of 2.5 obtained from (15); in some cases this ratio was less than unity, i.e. ionization in a linearly polarized field was more effective. Thus the results reported in Ref. 71 demonstrate that the ratio (15) fails to describe the multiphoton ionization of alkaline-earth atoms in the visible frequency range. This suggests that the most probable cause for the observed deviations from (15) lies with the multielectron effects, which are important in atoms with many electrons in the outer shell.

3.3. Excitation of two-electron states

Let us consider two-electron bound states. Several studies have reported resonances involving such states. For example, the three-photon ionization spectrum of barium[72] exhibits several resonance peaks which, by comparison with the atomic spectrum of Ba, cannot be attributed to anything else but three-photon resonances with two-electron bound states. The validity of this result is supported by the low nonlinearity order of the ionization process and the correspondingly low radiation field intensity of 10^6 V·cm^{-1} sufficient to create Ba^{2+} ions. At such low field intensities the perturbation of the atomic spectrum is small and does not exceed the linewidth of the observed resonances, which is of the order of several cm^{-1}. We should note, however, that in these experiments.[72] by no means all known two-electron bound states in the atomic spectrum of Ba appeared to participate in intermediate resonances. In a number of other alkaline-earth atoms no such resonances were observed.[72] Thus we can state that the currently available experimental data on the excitation of two-electron bound states are rather sketchy: beyond the fact that these states have been observed no additional physical conclusions can be drawn.

Now let us turn to the role of autoionizing states in the multiphoton ionization of atoms. Lasers have long been used in the spectroscopy of autoionizing states. However, in a typical spectroscopic experiment these states are excited in a multistep cascade by several laser frequencies, where each cascade step consists of a single-photon resonance transition. Consequently, the entire process can take place at fairly low field intensities $E \leqslant 10^4$ V·cm^{-1}. At the same time, the observation of a direct (nonresonance) multiphoton process (even in the limiting case of small nonlinearity order: $K = 2$, 3) requires field intensities that are higher by several orders of magnitude ($E \gtrsim 10^6$ V·cm^{-1}) than those sufficient for single-photon resonance excitation. Consequently, multiphoton ionization involves resonances with autoionizing states in much stronger radiation fields. Also, multiphoton resonances with autoionizing states can appear in the spectra of both singly and doubly charged ions. The key process is the decay of the autoionizing state. When this decay follows the classical channel (one electron moves to a lower energy state while another transfers to the continuum), the resonance should appear in the singly charged ion spectrum. When the decay involves the stimulated transition of two electrons into higher energy states and, eventually, into the continuum (by absorption of external field photons), the resonance should appear in the doubly charged ion spectrum.

A great number of studies have focused on the multiphoton ionization of atoms involving autoionizing states (see, for example, Refs. 70–77). The general case was treated by Andryushin and co-workers,[74,77] who also considered the stimulated transitions from autoionizing states to higher energy states.

Multiphoton resonances involving autoionizing states have been observed in singly charged ion spectra.[73,82–84]

Chin and co-workers[73] studied the three-photon ionization of strontium atoms and observed resonances in the Sr^+ ion yield corresponding to the three-photon excitation of 4d4f autoionizing states. Of greatest interest are the data obtained in this paper on the dependence of the shape of the resonances on the intensity of the exciting field which was varied from $3 \cdot 10^6$ to $1.5 \cdot 10^7$ V·cm^{-1}. At a low intensity of the field narrow resonances were observed at frequencies corresponding to known values of the energies of autoionizing states of the 4d4f series. At higher field intensities, these resonances became broader but their positions did not change (see Fig. 12), although in some cases neighboring resonances would merge into a broad resonance profile. As the field intensity reached $\approx 10^7$ V·cm^{-1} resonance broadening ceased to increase. A theoretical description of these experimental results within the framework of Andryushin's general model[74] was carried out by Kotochigova.[85] This analysis proposed the existence of two single-photon quasiresonances in the *Sr* spectrum at the working laser frequency—the quasiresonance between the $5p^2$ bound state and the autoionizing 4d4f states, and the quasiresonance between these 4d4f states and the autoionizing 6s7d states (see Fig. 12). The resonance mixing of these states then produced the observed broadening and saturation of the three-photon resonance with the 4d4f states at increasing field intensities.

At first sight, the experimental data of Refs. 83, 84 appear contradictory. Both experiments examined the frequency dependence of Xe^+ ion production in the three-photon ionization of xenon. The authors of Ref. 83 did not observe any resonances in the production of Xe^+ ions, but only some features in the electron angular distribution at the frequency corresponding to the calculated resonance with the autoionizing state of total angular momentum $J = 3$. In Ref. 84, on the other hand, sharp peaks in the formation of Xe^+ ions were indeed observed at points corresponding to three-photon resonances with a number of autoionizing states, in addition to features in the electron angular distributions. That experiment also found the resonance excitation efficiency to depend on the polarization. Currently, no explanation exists for the discrepancy between these two experiments.[83,84] We note that the results of the latter experi-

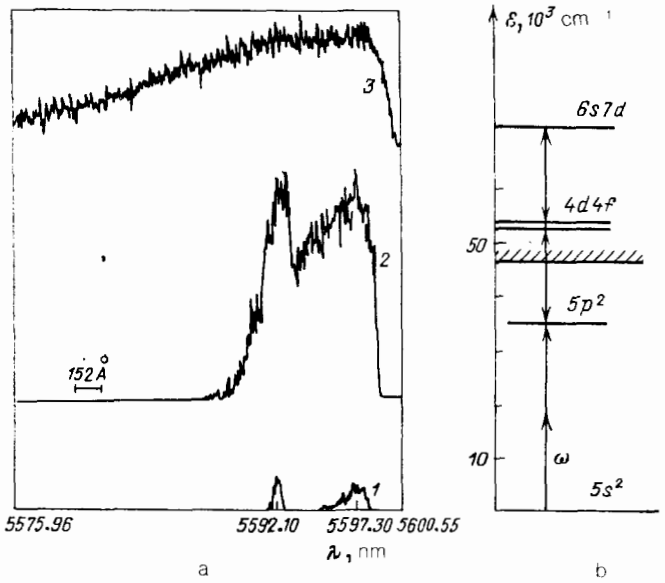

FIG. 12. a—Photoelectron yield in the three-photon resonance with the 4d4f autoionizing states as a function of radiation intensity: 1—$I = 3.6 \cdot 10^6$; 2—$I = 4.8 \cdot 10^6$; 3—$I = 9.4 \cdot 10^6$ W·cm^{-2}.[73] b—Schematic transition diagram.

ment[84] are in qualitative agreement with earlier theoretical calculations.[76]

Theoretical research into the effect of electromagnetic radiation on autoionizing states has paid much attention to the interference of various ionization channels.[74–78]

For instance, the transition to the continuum directly from the bound states interferes with the transition to the same continuum states via intermediate autoionizing states. These interfering channels coexist with other channels that do not contribute to interference effects—for example, the photoionization of autoionizing states. The role of various channels has been elaborated in several theoretical studies,[74,80] which concluded that the presence of noninterfering channels significantly modifies the final result. For example, the widely discussed phenomenon of the field-induced narrowing of autoionizing states[75,78] generally does not occur because of noninterfering channels.[74] An exception to this tendency is the mechanism treated in Ref. 79, where the noninterfering channels should not prevent the field-induced narrowing of autoionizing states, although they would still affect this process.[74]

There has been some discussion of another mechanism for the narrowing of autoionizing states: the resonance mixing of broad autoionizing state multiplets with narrow discrete levels.[81] According to this mechanism[81] the width of the resulting quasienergetic states could be quite narrow because of the large contribution of the wavefunctions corresponding to narrow discrete levels.

The above discussion indicates that general theoretical models dominate this interesting research topic, while concerted experimental efforts are lagging behind.

3.4. Excitation of forbidden states

A number of experiments investigating the multiphoton ionization of alkaline-earth atoms have observed, in addition to the allowed intermediate multiphoton resonances involving the singlet states, a number of forbidden resonances between the ground state singlet and the excited triplet states. Moreover, the amplitude of the forbidden resonances was of the same order as the amplitude of the allowed resonances. An analogous effect was observed in the Rydberg states ($n > 12$) of alkaline-earth atoms, where it was explained by configurational mixing in the Rydberg state spectrum.[86]

Obviously, the mechanism by which the forbidden transitions between states with low principal quantum numbers give rise to resonances is of great interest. Indeed, these are the states that usually dominate the various multiphoton processes. Alimov and co-workers[87] studied the three-photon ionization of three alkaline-earth atoms—strontium, barium, and calcium—in a wide range of tunable laser frequencies. They observed both allowed and forbidden intermediate two-photon resonances with states of different principal quantum numbers. This experiment demonstrated that the excitation efficiency of forbidden resonances depends on the principal quantum number of the excited state (Fig. 13). Furthermore, the observed behavior correlates with the known dependences for the quantum defect (see Fig. 13). This correlation lends further credence to the importance of configurational mixing. We should note that while the configurational mixing in the Rydberg states is well described by

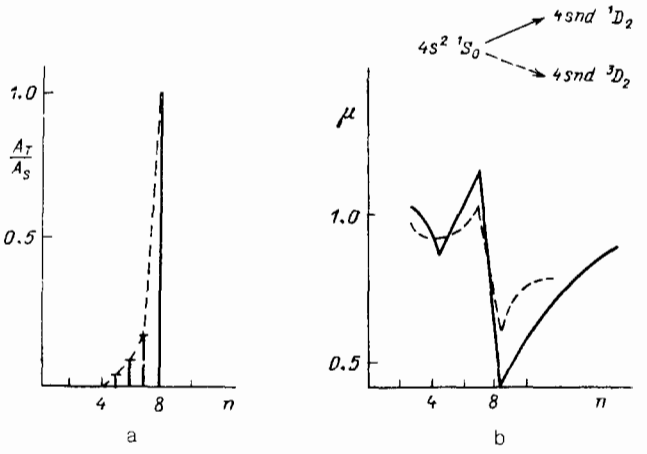

FIG. 13. a—Ratio A_T/A_S of ion yields in the three-photon ionization of Ba for intermediate two-photon resonances with the triplet (T) and singlet (S) states as a function of the principal quantum number n of these states.[87] b—Dependence of the quantum defect μ on n.

the theory of the multichannel quantum defect, there exists no consistent theoretical description of configurational mixing in the lower excited levels.

Let us also mention an experiment[88] which recorded two-photon resonances forbidden by the orbital angular momentum selection rules, and another experiment[89] which observed the single-photon excitation of the quadrupole transition.

In sum, we can state that many-electron effects have been observed both in the multiphoton resonance ionization of alkaline-earth atoms and in their direct ionization.

3.5. Angular distributions of photoelectrons

We know that the angular distributions of electrons emitted during multiphoton ionization contain valuable independent information on both the direct and the resonance ionization processes.[2,3] In the direct process, the atomic properties manifest themselves in the coefficients of the even cosine powers of the electron exit angles. In the resonance processes, the electron angular distribution is determined by the intermediate resonance states.

The very first experiments studying the angular distributions of electrons emitted during multiphoton ionization of alkaline-earth atoms[90] demonstrated that the single-electron classification of bound states fails to describe adequately their complex nature, which is actually determined by configurational mixing. Subsequently, the barium atomic system was subjected to the greatest scrutiny.[91] In these experiments, after exciting the barium atoms into various preselected states with a laser, the researchers would monitor the photoionization of these states, recording the angular distribution of emitted electrons. The main achievement of these experiments was the observation of configurational mixing among the bound states. In some cases it was possible not only to identify the states participating in the configurational mixing, but also to estimate their relative contributions. For example, the angular distributions of electrons emitted during the photoionization of several neighboring barium states were compared with theoretical calculations to determine that photoionization can leave the barium ion

TABLE II. Probabilities of finding the Ba^+ ion in the various final states (6s, 5d, $6p_{1/2}$, $6p_{3/2}$) in the cascade ionization of Ba via the intermediate $6p^2\ ^3P_1$ and $6p^2\ ^3P_2$ excited states. These results are obtained from an analysis of experimentally measured angular distributions of emitted electrons.

	6s + 5d	$6p_{1/2}$	$6p_{3/2}$
$6p^2\ ^3P_1$	13 %	33 %	54 %
$6p^2\ ^3P_2$	14 %	13 %	73 %

in any one of four states: 6s, 5d, $6p_{1/2}$, and $6p_{3/2}$. The relative probabilities of transitions into these states are cited in Table II. Clearly, all these bound states consist of superpositions of different states with different angular momenta and hence the standard single-electron classification of these states employed in the first column of Table II does not reflect their true complexity.

3.6. Conclusion

The above analysis of the various effects observed in the multiphoton ionization of alkaline-earth atoms leads to two conclusions. First, all the differential characteristics of the multiphoton ionization process (frequency resonances, polarization dependences, electron angular distributions) reflect the many-electron structure of the bound state spectrum (configurational mixing, two-electron states). Second, the integral characteristics of multiphoton ionization (multiphoton cross sections of the direct ionization process) are generally similar to their counterparts in systems with a single optical electron.

Unfortunately, no experimental data analogous to the alkaline-earth data are available for other atomic groups in the periodic table. We can hypothesize, however, that the ionization of atoms with several equivalent electrons in the outer shell also would exhibit many-electron effects.

Finally, if we consider multiphoton ionization as a means of investigating atomic structure, it appears that the combination of resonance ionization with electron spectroscopy provides us with a uniquely flexible tool in the study of the complex electronic state structure of atoms with many optical electrons. The theoretical description of many-electron effects requires a complex mathematical treatment. The most promising approach appears to employ the density functional and the random phase approximation with exchange. For an example of a successful application of these methods to the problem of multiphoton transitions in the many-electron approximation, we can point to Refs. 92–96.

4. FORMATION OF MULTIPLY CHARGED IONS

After the publication of Ref. 12, where the formation of doubly charged ions was first reported, many experiments have focused on the formation of multiply charged ions. The main conclusion arising from the totality of these experiments is that multiply charged ions are produced in multielectron atoms by all types of nonlinear ionization processes, regardless of the radiation frequency (from infrared to ultraviolet), the atomic species, or the limiting case of the process (whether multiphoton $\gamma \gg 1$ or tunneling $\gamma \ll 1$). Beginning with the first experiments, the main unknown in this process was whether the formation of multiply charged ions occurred by a direct or a cascade process. Currently, the cascade process[97,98] is generally accepted as the actual mechanism responsible for the creation of multiply charged ions. In the simplest reaction, leading to the production of a doubly charged ion, the cascade process appears as

$$A + K_1\omega \rightarrow A^+ + e, \quad A^+ + K_2\omega \rightarrow A^{2+} + e,$$

whereas the direct process follows

$$A + K_3\omega \rightarrow A^{2+} + e + e.$$

In the case when the produced ions have a charge q^+, the cascade process consists of q steps qualitatively analogous to the single cascade step described above.

In fact, the identification of the observed formation of multiply charged ions with either a direct or a cascade process is far from a simple matter. The cascade reaction cited above is a simplification. First, as an electron is emitted, the remaining ion need not remain in the ground state. Consequently, the next step in the cascade could involve electron emission from an excited ion. Second, intermediate resonances may enter into both direct or cascade processes. Third, the ionization process could saturate at some of the transitions (when $w\tau_1 \sim 1$, where w is the probability of ionization per unit time and τ_1 is the duration of the laser pulse). For these reasons the description of multiply charged ion formation in terms of such integral characteristics as the nonlinearity order of the A^{q+} ion formation ($\partial \lg A^{q+}/\partial \lg I$), the total probability of A^{q+} ion formation per laser pulse, etc., is fraught with difficulties and usually yields no definitive conclusions. The most reliable information on the formation mechanism is obtained from the resonances in the ion yield, which can be compared with resonances in the atomic and ionic spectra, and from the analysis of the energy spectrum of emitted electrons which can establish the final state of the end-product ions. As we shall see, this type of experimental information has made it possible to develop a fairly reliable description of the formation of multiply charged ions.

The central problem in the theoretical analysis of the cascade process consists of calculating the multiphoton cross-sections for electron emission and their dependence on the radiation frequency. Here, traditional methods developed for the description of the multiphoton ionization of atoms[2,3] can be brought to bear. By calculating the multiphoton cross-sections in the ionic spectrum, as well as saturation effects, it becomes possible, in principle, to describe quantitatively the ratios between the formation of differently charged ions. However, as we have already seen, actual multiphoton cross-sections can be calculated only in the single-electron approximation, whose validity in this case is questionable.

In a relatively weak field, perturbation theory tells us that the probability of the direct K-photon process is largely determined by the component matrix element of order K. If $K \geqslant q$, all the single-photon matrix elements can be calculated in the single-electron approximation. When correlation effects are ignored these matrix elements turn out to be nonzero, so in this sense the existence of the direct K-photon

channel for q-electron ionization ($K \geqslant q$) elicits no doubts. Yet the calculation of these matrix elements is difficult, as it involves summation over intermediate states which could include multielectron excited states as well as autoionizing states. A number of models[99–108] have been developed to overcome these difficulties and compute the absorption of field energy by the atom as a whole and the emission of many electrons. We shall omit a detailed analysis of these models for two reasons: first, they all contain some *a priori* assumptions without the required justifications; second, they all introduce several fitting parameters which formally assure agreement with experimental results. A brief review of these models is available in Ref. 97.

Now let us turn to the experimental data and their analysis. Many studies devoted to the formation of multiply charged ions have been published since the pioneering work of Crance.[12] In keeping with the style of this review, we shall neither cite nor comment on all these studies, but rather discuss those which we believe to have uncovered significant new results.

On the basis of the parameters characteristic of the studied atoms and ions, and the frequency and intensity of the radiation field, we can group all the available experimental results into the following categories:

4.1. Formation of doubly charged alkaline-earth ions by visible or near IR radiation

The results of numerous experiments devoted to this process clearly indicate that in the visible spectral range the process has a cascade character. In order to prove this assertion we shall call on the results of the three most convincing experiments.

The formation of singly or doubly charged ions of Ca, Sr, and Ba atoms by radiation in a wide 15000–18700 cm^{-1} frequency range (with linewidths of 2–3 cm^{-1}) was observed in Ref. 109. In that frequency range the single-electron ionization of all atoms required three or four photons. The formation of doubly charged ions was observed in a radiation field of 10^5–10^6 $V \cdot cm^{-1}$ intensity, i.e. the shifts in the bound state energy levels due to the dynamical Stark effect were fairly slight and did not exceed the laser linewidth.

Many resonances have been observed in the radiation frequency dependence of doubly charged ion formation. These resonance frequencies (numbering several tens) have been compared with reference data on the single-electron states of singly charged ions, as well as with the spectra of two-electron states of the studied atoms. In the overwhelming majority of the cases, the ion formation resonances would agree within the laser linewidth with the transitions in the singly charged ion spectra allowed by the multiphoton transition selection rules. These multiphoton transitions originated both from the ground and first excited states of singly charged ions. Resonances which could be identified with two-electron bound states of the atoms under discussion were also observed, but in much smaller numbers.

Thus the main conclusion arising from these experiments has been that the cascade process is the dominant mechanism in the formation of doubly charged ions. We should note that this conclusion appears quite general, as it applies to experimental results in all three atomic systems—barium, strontium, and calcium.

The data of Ref. 110 have furnished additional important information on the formation mechanism of doubly charged ions. In that experiment the authors monitored the energy spectrum of emitted electrons in the three-photon ionization of strontium by radiation tunable in the 17400–17900 cm^{-1} frequency range. The field intensity was $E \approx 10^7$ $V \cdot cm^{-1}$. The frequency dependence of electron emission, which contained sharp resonances, was combined with the electron energy spectrum to identify the various channels leading to the formation of doubly charged ions by cascade ionization. A schematic diagram of the alternative channels is illustrated in Fig. 14.

With the electron spectroscopy data in hand, we can now look back at the experimental data monitoring ion formation only (for example, Ref. 109) and observe that the formation of doubly charged ions at some fixed frequency comprises the contribution of several ionization channels. This implies, in particular, that the functional dependence of ion formation on radiation intensity ($\partial A^{2+}/\partial I$) between the resonances should not conform to a power law (as it does in a direct multiphoton process). This explains why many earlier experiments found that the intensity dependence $\partial A^{2+}/\partial I$ cannot be approximated by a power law.

The experiment of Eichmann and co-workers[111] employed the radiation of three dye lasers, which made it possible to ionize barium atoms by a cascade process in such a way that the Ba^+ ion could be selectively produced in either the ground or the excited state. In this experiment intense laser radiation in the 560–610 nm wavelength range would produce doubly charged barium ions both with and without preliminary irradiation of the atomic Ba species. It was discovered that the amplitude of the resonance peaks in the production of Ba^+ ions is affected by preliminary irradiation. The experimental data demonstrated directly that the formation of Ba^+ ions proceeds by a cascade process: more precisely, the Ba^+ ions are created in the $6S_{1/2}$, $5D_{1/2}$ and $5D_{3/2}$ states; then, in a separate cascade step, the electrons are removed from the Ba^+ ions to create the doubly charged species.

Consequently the more successful experiments have established clearly that the production of doubly charged ions proceeds by a cascade process.

We should note that currently there is no indication as to which concrete mechanism creates ions in the excited state. The only definite statement one can make is that this mechanism is many-electron in character.

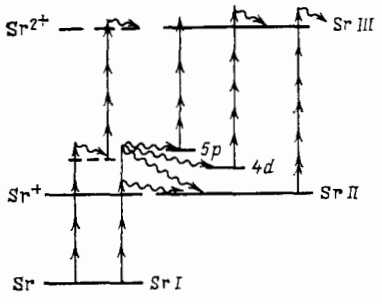

FIG. 14. Transition diagram illustrating the formation of singly charged Sr^+ ions in the ground and excited states. These data were obtained by electron spectroscopy.[110]

Finally, let us return to the question of the relative formation efficiencies of the singly and doubly charged alkaline-earth ions. Evidently, in the case of a cascade process, saturation effects should make the production of ions with charge q only slightly less efficient than the production of ions with charge $q-1$, and typically this is confirmed by the experimental data.

Experiments in the near IR range ($\omega \sim 1$ eV) are less complete and generally less reliable. On the one hand, the data of Ref. 112 do point to a cascade process. On the other hand, from the very first experiments[113] onward, the measured amplitudes of singly and doubly charged ion formation have been difficult to reconcile with the available information on multiphoton cross sections. (This problem does not occur in ionization by radiation in the visible range, where the difference in the nonlinearity orders between ionization of the atom and electron removal from a singly charged ion is smaller). Additional experiments, including electron spectroscopy measurements, are required.

In conclusion, we note that the formation of triply charged calcium ions have been observed in similar (ω, E) experimental conditions.[114] Consequently, electrons can be removed from the inner atomic shells, as well as the outer.

4.2. Formation of multiply charged noble gas ions by visible and near IR radiation

The main achievement of the experiments investigating the formation of multiply charged noble gas ions by near infrared[115] and visible[116] radiation has been the observation of ions with large charge multiplicities, up to six in uranium (U^{6+} ions). In these experiments the radiation field intensity was in the 10^8–10^9 V·cm^{-1} range, higher than the intensity necessary to ionize alkaline-earth atoms (although even these high fields are considerably weaker than the atomic field). The ionization was accomplished at the fundamental frequency of the neodymium glass laser ($\omega \approx 1.2$ eV) and its second harmonic ($\omega \approx 2.4$ eV). Since the laser frequency was fixed, in addition to the existence of multiply charged ions, L'Huller and co-workers[115,116] were only able to measure the intensity dependence of the ion production. From this intensity dependence the authors of Refs. 115, 116 drew several conclusions about the mechanism of doubly charged ion formation (the presence of both direct and cascade ionization processes, and their relative contributions). However, by analogy with the information on second ionization in the alkaline-earth atoms furnished by electron spectroscopy, we can expect that many ionization channels also contribute to the ionization of noble gas atoms and hence the interpretation of $\partial A^{q+}/\partial I$ is far from unambiguous. This became clear in the course of continuing electron spectroscopy measurements by the same research group.[117] As in other experiments on different systems, measurements of the energy spectrum of emitted electrons reported in Ref. 117 contained peaks due to above-threshold absorption. The fixed frequency and high intensity of the radiation field used in these measurements hinder the comparison with atomic and ionic spectra, however, and no definite conclusions about the mechanism of multiply charged ion formation can be drawn.

To sum up this series of experiments, the authors have observed multiply charged ions produced by near IR radiation at field intensities smaller than the atomic field. No definitive statements about the physical mechanism behind this process can be extracted from the experimental data. However, the intensity dependence of the multiply charged ion yield measured in these experiments is characteristic of cascade ionization and hence we believe that this mechanism is dominant in these atomic systems.

Perry and co-workers[118] studied the multiple ionization of noble gas atoms in the field of a dye laser working in the 10^{13}–$4\cdot10^{14}$ W·cm^{-2} intensity range at $\lambda = 586$ nm. An interesting result of this research was the observed dependence of the threshold intensity for the creation of various multiply charged ions (defined as the intensity at which the appropriate ionization probability reaches 10^{-4}) on the atomic and ionic ionization potentials. All the experimental data for different atoms and ions can be described by a single smooth curve (Fig. 15). According to the authors of Ref. 118 this single dependence indicates that the ionization probability is largely determined by such macroscopic characteristics of atoms and ions as the ionization potential and is only weakly related to their internal structure. At first sight it appears that these experimental results (see Fig. 15) and their interpretation contradict our models wherein intermediate resonances enhance the ionization probability. Indeed, given such a large number of systems as several atoms and their variously charged ions, intermediate resonances should appear in at least some systems. The possible reasons for the absence of such resonances are two: strong broadening of resonances and their large field-induced shift. In the experimental conditions of Ref. 118 both the dynamical Stark shift of the atomic levels and the single-photon ionization broadening reach the magnitude of several eV. Hence a distinction between direct and resonance ionization processes is no longer possible.

4.3. Formation of multiply charged ions by UV radiation

Ionizing UV radiation at several frequencies and quantum energies in the 4.0–6.5 eV range has been used to ionize various atoms. The field intensity employed in these experiments ranged from lower than the atomic field, to being of the same order or even an order of magnitude greater. These experiments have observed the removal of the largest number of electrons from an atom (eight electrons from uranium) which required the absorption of up to 600 eV, i.e. up to 100 photons. By ionizing atoms with various outer shell structures, from alkali atoms to noble gas species, multiply charged ions were produced.[119–121] The main result of these experiments has been the determination that multiply

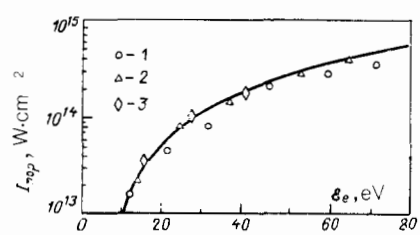

FIG. 15. Threshold intensity I_{th} for the formation of multiply charged ions as a function of electron binding energy ε_{bind} to the ion.[118] 1—Xe; 2—Kr; 3—Ar ions.

charged ions with relatively low charge multiplicities can be created by cascade processes in fields of lower intensity than the atomic field.

Johann and co-workers[120] have studied the creation of multiply charged noble gas ions by UV radiation with 6.4 eV quantum energy and field intensity in the $3\cdot10^8$–10^9 V·cm^{-1} range. They reported data on the electron yield as a function of electron energy in the 0.3–100 eV interval. These electron spectra exhibit sharp peaks whose relative amplitude depends on the field intensity (Fig. 16). By comparing the energies corresponding to peaks in the electron spectra with the spectra of ionized atoms and their charged ions we can arrive at three conclusions: above-threshold ionization is observed both in atoms and atomic ions; the relative amplitude of processes involving the absorption of different numbers of photons changes as a function of field intensity; both the ground and the excited ionic states can be ionized.

For a concrete example consider the reaction in which the Xe^{3+} ion is created by removing an electron from Xe^{2+}:

$$Xe^{2+} + (6\omega;\ 7\omega;\ 8\omega) \rightarrow Xe^{3+} + e;\ (Xe^{3+})^* + e.$$

The experimentally observed peaks in the electron distributions corresponding to these three reactions are, respectively:

$$\mathcal{E}_{e,\,kin} = \mathcal{E}^{(0)}_{e,\,kin} = 6{,}3 \text{ eV},\ \mathcal{E}^{(0)}_{e,\,kin} + \omega = 12{,}8 \text{ eV},$$

$$\mathcal{E}^{(0)}_{e,\,kin} + 2\omega = 19.2 \text{ eV}.$$

As we have mentioned already, the actual mechanism that creates ions in the excited state is at present not known.

As a whole, these experimental results indicate that the formation of ions with charge multiplicities up to three proceeds via a cascade process. There are grounds for conjecturing that ions with higher charge multiplicities are created by cascade ionization as well. The temporal evolution of the creation of multiply charged Xe^{q+} ions by a 0.5 ps laser pulse with $\lambda = 248$ nm and peak intensity $I_{max} = 10^{16}$ W·cm^{-2} (Fig. 17) was reported in Ref. 121. It follows from this figure that the formation of Xe^{q+} ions is nearly always preceded by the saturation of $Xe^{(q-1)+}$ ion formation, as would be expected if many-electron ionization occurs by a cascade process.

Finally, let us mention the many theoretical studies (for example, Refs. 104–106) devoted to the interpretation of the experimental data on the ion yield as a function of charge multiplicity reported in Ref. 120, as well as in earlier studies of the same research group. In particular, there have been

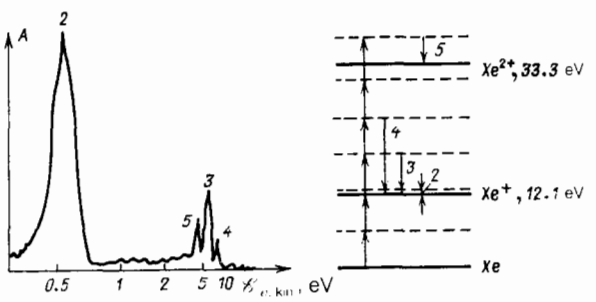

FIG. 16. Energy spectrum of electrons created in the course of Xe^+ and Xe^{2+} ion formation in a UV radiation field.[120] The numbers 2–5 label some of the reaction channels and the corresponding spectral peaks.

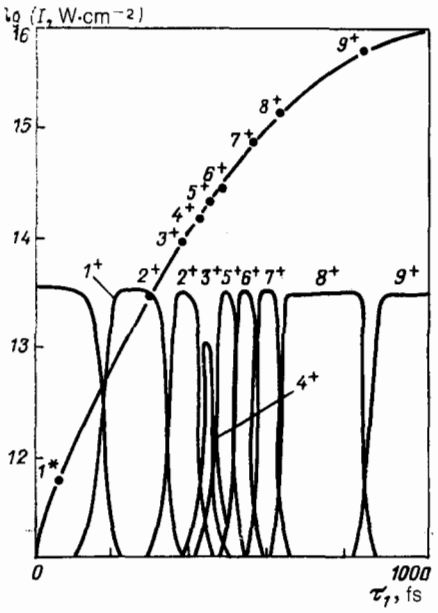

FIG. 17. Dynamics of the cascade ionization of XE in a single laser pulse.[121] The numbers q on the pulse envelope mark the threshold intensities for the formation of ions with charge multiplicity q. The curves below illustrate the formation of q^+ ions as a function of time.

suggestions that these experimental data support the existence of many-electron processes in the absorption of radiation by the atom and (or) emission of an electron by an excited atom. We believe these suggestions to be unfounded, for the following reasons. First, the results of the aforesaid experiment[120] furnish clear evidence that the creation of ions with charge multiplicity up to three proceeds by a cascade process. Second, the distribution of ions as a function of their charge multiplicity was experimentally measured at radiation intensities in the 10^{15}–10^{17} W·cm^{-2} range, that is at field intensities from 10^9 to 10^{10} V·cm^{-1}, i.e. at $E \gtrsim 1$. At such high external fields, treating the atom or, more precisely, the entire electron shell of the atom as a single system requires separate justification.

Thus, in summing up all the available experimental data on the formation of multiply charged ions by UV radiation, the only reliable conclusion is that at field intensities $E < 1$ the formation of ions with charge multiplicities up to three proceeds by a cascade process.

4.4. Conclusion

In all, what are the general and reliable conclusions that can be drawn about the formation of multiply charged ions using laser irradiation?

First, a laser field of any frequency, from IR to UV, will create multiply charged ions of any complex atom once sufficient field intensities are attained.

Second, cascade processes dominate the formation of multiply charged ions at all frequencies. Each step of the cascade consists of a direct or resonant multiphoton ionization process. When individual cascade steps become saturated, the yield of ions with charge multiplicity q reaches the same order of magnitude as the yield of ions with multiplicity $q-1$.

Third, the final state of the ion created by cascade ionization need not be the ground state—ions can be created in an excited state as well.

5. THE TUNNEL EFFECT IN A TIME-VARYING FIELD

We have already mentioned that research into the nonlinear ionization of atoms has been going on for over 20 years. Until recently, however, all experimental studies concentrated on the multiphoton limiting case ($\gamma \gg 1$), not by virtue of a deliberate experimental strategy, but rather because of technical difficulties that hindered the generation of sufficiently intense fields in the infrared. Yet only in the infrared frequency range was it possible to reach the tunneling limiting case ($\gamma \ll 1$) for the ionization of atoms from the ground state in fields of intensity $E \ll 1$. With the advent of powerful pulsed CO_2 lasers, operating in the infrared ($\lambda \approx 10$ μm, $\omega = 0.1$ eV), as well as the materials required for focusing infrared radiation, researchers seized the opportunity to study the ionization process in the tunneling limiting case.[122,123]

In these experiments radiation froma CO_2 laser was focused on Xe atoms in a gaseous phase, maintained at $\sim 10^{-6}$ torr. Ionization was observed in the 10^{13}–10^{14} W·cm^{-2} intensity range, producing singly and multiply charged Xe ions (up to Xe^{6+}). A comparison of the field intensity, radiation frequency, and the binding energies of the electron to the atom and the various ions demonstrated that in all cases the adiabaticity parameter was $\gamma \sim 10^{-2} \ll 1$. Consequently these experiments have observed tunneling ionization in a time-varying field. This conclusion was corroborated by the results of a control experiment[122] in which two different wavelengths, $\lambda = 9.55$ μm and $\lambda = 10.55$ μm, were employed for ionization. At these wavelengths, the yields of Xe^+ and Xe^2 ions as a function of radiation intensity turned out to be identical, confirming the original hypothesis that ionization proceeds by tunneling in these conditions. Finally, it is worth noting that the ion yields of different charge multiplicities as a function of radiation intensity followed the well-known dependence characteristic of cascade ionization.

Consequently, these experiments[122,123]demonstrated that ionization does take place in the tunneling limiting case ($\gamma \ll 1$) and that the formation of multiply charged ions occurs by a cascade process.

The experimental data agree with theoretical calculations. Clearly the results of these experiments cannot be described by the well-known formula[2] for the probability of tunnel ionization in a time-varying field, which is only valid for the hydrogen atom. More sophisticated formulae are required, incorporating the ionization potential of complex atoms, changes in the ionization potential due to the dynamical Stark effect, the ionic charge, and the nonmonochromatic nature of a real laser beam. A comparison of calculations performed in Ref. 124, which took into account the real ionization potential and ionic charge, with the experimental data[122,123] on the ionization of Xe atoms and ions with charge multiplicities of one through three, demonstrates adequate agreement of theory and experiment.

We emphasize that the results reported in Refs. 122 and 123 constitute a major advance in nonlinear ionization research, because they confirm the validity of the fundamental hypothesis on the existence of a single ionization process with two limiting cases—the multiphoton and the tunneling cases. However, these results are only preliminary and further experimental and theoretical studies of the ionization of atoms with the adiabaticity parameter $\gamma \ll 1$ are necessary.

6. GENERATION OF RADIATION AT SHORTER WAVELENGTHS

The above-discussed experimental data pertaining to the formation of multiply charged ions indicate that these ions are created in excited states, as well as the ground state. This implies the possibility of fluorescence according to the following scheme, which is an extension of the previously discussed reaction (14):

$$A^{(q-1)+} + K_i\omega \to (A^{q+})^* + e, \quad (A^{q+})^* \rightsquigarrow A^{q+} + \nu. \quad (16)$$

If the charge multiplicity q of the ion is high, the fluorescence radiation ν can lie in the short wavelength region.

Radiation at vacuum UV frequencies was observed from noble gas atoms irradiated with a pulsed UV laser (at intensities of 10^{13}–10^{14} W·cm^{-2}). This experiment differed from nearly all other studies in that the gas flow was pulsed. The density of the irradiated gas in the focus spot of the laser beam reached up to 10^{18} per cm^3. The extremely short duration of the laser pulse ($\sim 10^{-12}$ s) meant that the particles in the irradiated volume did not have time to collide. The observed radiation frequencies corresponded to various transitions in the ionic spectra, including transitions between different shells. The shortest recorded fluorescence wavelength was 12 nm ($\omega \sim 10^2$ eV). The effective cross sections for fluorescence at $\lambda \sim 18$ nm from Xe^{7+} and Kr^{7+} was estimated from the experimental data to be of the order of 10^{-24} cm^2.

In addition to short wavelength lines identified with fluorescence, this experiment yielded the observation of higher odd optical harmonics of the excitation beam. The highest degree of nonlinearity in the transformation of laser radiation was recorded in neon, where the 17th harmonic was observed ($\lambda \sim 14$ nm, energy quantum $\sim 10^2$ eV, effective cross section $\sim 10^{-29}$ cm^2). The harmonic generation efficiency at first dropped quickly with higher harmonic order and then more slowly as higher order harmonics were reached.

Subsequently the excitation of higher harmonics was observed when noble gas atoms were irradiated in the near IR ($\omega \approx 1$ eV) with intensities of about 10^{13} W·cm^{-2}.[126] This experiment also employed a pulsed gas flow. The highest degree of nonlinearity was recorded in argon, where the 33rd harmonic was observed ($\lambda \sim 32$ nm, energy quantum ≈ 40 eV). The harmonic generation efficiency as a function of harmonic order in Ar is shown in Fig. 18. Qualitatively identical dependences were observed in other atoms.

A theoretical treatment of the excitation of higher optical harmonics in circumstances where the harmonic energy quantum far exceeds the atomic ionization potential was attempted in Refs. 127 and 128, whose authors proposed that this process is related to the above-threshold ionization effect. An alternative interpretation could involve the excitation of higher harmonics in the spectra of multiply charged ions, where the harmonic energy quantum is smaller than the electron binding energy.

Clearly these recently discovered phenomena are of great scientific and practical interest.

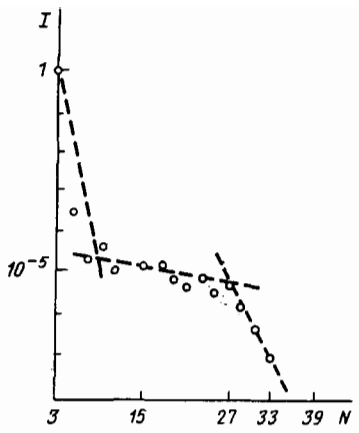

FIG. 18. Relative intensity I of higher harmonics generated in gaseous Ar excited by an infrared laser beam ($\omega \approx 1.2$ eV) as a function of harmonic order N of the harmonic).[126]

7. GENERAL CONCLUSION

In summing up the new effects in the nonlinear ionization of atoms by a time-varying electromagnetic field discovered and investigated in recent years, we believe the most important advance has been the discovery of above-threshold ionization. Another important advance has been the conclusion that in the multiphoton limiting case ($\gamma \ll 1$) the applicability region of time-dependent perturbation theory is bounded not by the condition that the field intensity E be smaller than the atomic field (e.g. $E < 1$), but rather by more stringent conditions $E \ll 1$. The experimental data cited above indicate that this fundamental result applies not only to atoms, but also to atomic ions and molecules.

Another important new effect is the formation of multiply charged ions. All the currently available information on the formation mechanism of multiply charged ions appears to support a cascade process. Currently there is no unambiguous evidence in favor of the direct many-electron process, which would be of fundamental physical interest.

Finally, an important conclusion that follows from any of the experiments devoted to the multiphoton ionization of alkaline-earth ions is that both of the outer shell electrons play an important role in this process. The same conclusion also follows from the analysis of the formation mechanism of doubly charged alkaline-earth ions.

We should also say a few words about ultra-high field intensities. Earlier we mentioned that field intensities of $E > 1$ are available today and that ionization processes have already been observed in such fields. More importantly, we are currently on the brink of a new era of ultra-high field intensities, which are becoming attainable not by virtue of hypertrophied laser designs, but rather by pulse compression available at the expense of line broadening. Even now, one can obtain field intensities significantly higher than the atomic field by compressing picosecond pulses into the femtosecond range. Not only will the advent of ultra-high intensity fields open the door to new effects, such as the light-induced creation of electron pairs in the field of the nucleus and in vacuum, but also to new opportunities in the nonlinear ionization of atoms. Recall that the ionization process at $E > 1$ is fully understood only in a static field, where ionization becomes time-independent. A time-varying field with $E > 1$ presents a number of unsolved problems.[2,4]

Progress in experimental techniques has created another new research field: the investigation and description of nonlinear ionization by ultrashort laser pulses.[129] The availability of femtosecond laser pulses has created a qualitatively new situation, when the interaction period with the external field becomes comparable to the time of revolution of an electron about the nucleus, and the pulse train becomes comparable to the radiation wavelength.

Finally, turning to practical applications, several advances have been achieved in recent years. For example, Zhang and co-workers[130] have reported stimulated emission in Mg vapor due to multiphoton processes in atoms and molecular dimers; Boyer and co-workers[131] have reported the generation of short wavelength stimulated emission in Kr based on an inter-shell transition; we have already discussed optical harmonic generation at extremely high harmonic orders, as well as fluorescence in ionic spectra which can be employed in generating vacuum UV radiation. These first results underscore the promise of multiphoton processes in complex atoms and at very high field intensities.

[1)] The atomic system of units shall be used throughout this review.

[1]V. A. Kovarskiĭ, Multiquantum Transitions (in Russian), Shtiintsa, Kishinev, 1974.
[2]N. B. Delone and V. P. Krainov, Atoms in Strong Light Fields, Springer-Verlag, N. Y., 1985 [Russ. original, Atomizdat, M., 1978; reissued Énergoizdat, M., 1984].
[3]L. P. Rapoport, B. A. Zon, and N. L. Manakov, *Theory of Multiphoton Processes in Atoms* (in Russian), Énergoizdat, M., 1985.
[4]M. Mittleman, *Introduction to the Theory of Laser-Atom Interactions*, Plenum, N. Y., 1982.
[5]*Multiphoton Ionization of Atoms* (ed. by S. Chin and P. Lambropoulos), Acad. Press, Toronto, 1984.
[6]V. A. Kovarskii, N. F. Perel'man, and N. Sh. Averbukh, Multiquantum Processes (in Russian), Énergoizdat, M., 1985.
[7]N. Manakov, V. Ovsyannikov, and L. Rapoport, Phys. Rep. **141**, 320 (1986).
[8]F. Faisal, Multiphoton Processes, North-Holland, Amsterdam, 1987.
[9]N. B. Delone, Usp. Fiz. Nauk **115**, 361 (1975) [Sov. Phys. Usp. **18**, 169 (1975)].
[10]Multiphoton Ionization of Atoms (in Russian), Nauka, M., 1980 (Trudy FIAN SSSR, Vol. 115 [Pror. (Tr.) P. N. Lebedev Phys. Inst. **115** (1980)].
[11]J. Morellec, D. Normand, and G. Petite, Adv. Atom. Mol. Phys. **18**, 98 (1982).
[12]M. Crance, Phys. Rep. **144**, 119 (1987).
[13]I. P. Zapesochnyĭ and V. V. Suran, Pis'ma Zh. Tekh. Fiz. **1**, 973 (1975) [Sov. Tech. Phys. Lett. **1**, 420 (1975)].
[14]P. Agostini, F. Fabre, G. Mainfray, G. Petite, and N. Rachman, Phys. Rev. Lett. **42**, 1127 (1979).
[15]N. B. Delone, V. P. Kraĭnov and D. L. Shepelyanskiĭ, Usp. Fiz. Nauk **140**, 355 (1983) [Sov. Phys. Usp. **26**, 551 (1983)].
[16]G. Casati, B. V. Chirikov, D. L. Schepelyansky (Shepelyanskiĭ), and F. Guarneri, Phys. Rep. **154**, 78 (1987).
[17]G. Casati, F. Guarneri, and D. L. Schepelyansky (Shepelyanskiĭ), IEEE J. Quantum Electron. **QE-24**, 1420 (1988).
[18]L. D. Landau and E. M. Lifshits, Electrodynamics of Continuous Media, 2nd Ed., Pergamon Press, Oxford, 1984 [Russ. original, Nauka, M., 1982].
[19]M. V. Ammosov, F. A. Il'kov, and Ch. K. Mukhtarov, Preprint Inst. Gen. Phys. Acad. Sci. USSR No. 79 (In Russian) M., 1985. M. V. Ammosov and M. V. Malakhov, Preprint Inst. Gen. Phys. Acad. Sci. USSR No. 273 (In Russian) M., 1988.
[20]G. Petite, P. Agostini, and F. Yergeau, J. Opt. Soc. Am. B **4**, 765 (1987).
[21]L. A. Lompre, A. L. L'Huillier, G. Mainfray, and C. Manus, J. Opt. Soc. Am. B **2**, 1906 (1985).
[22]A. Guisti-Suzor and A. Zoller, Phys. Rev. A **36**, 5178 (1987).
[23]S. Chin, C. Rolland, P. Corcum, and P. Kelly, Phys. Rev. Lett. **61**, 153 (1988).

[24]H. G. Muller, H. B. van den Linden van den Heuvell, and M. J. van der Wiel, Phys. Rev. A **34**, 236 (1986).
[25]E. Karule, in: Electronic and Atomic Collisions (Eds.) H. B. Gilbody, W. R. Newell, F. H. Read, and A. C. H. Smith), North-Holland, Amsterdam, 1988, p. 569.
[26]H. J. Humpert, H. Schwier, R. Hippler, and O. H. Lutz, Phys. Rev. A **32**, 3787 (1985).
[27]D. Feldman, B. Wolff, M. Wenhöner, and K. H. Welge, Z. Phys. D **6**, 293 (1987).
[28]Y. Gontier, N. K. Rahman, and M. Trahin, Europhys. Lett. **5**, 595 (1988).
[29]T. J. McIlrath, P. H. Bucksbaum, R. R. Freeman, and M. Bashkansky, Phys. Rev. A **35**, 4611 (1987).
[30]R. R. Freeman, P. H. Bucksbaum, H. Milchberg, S. Darack, D. Schumacher, and M. F. Censic, Phys. Rev. Lett. **59**, 1092 (1987).
[31]H. G. Muller, H. B. van den Linden van den Heuvell, P. Agostini, G. Petite, A. Antonetti, M. Franco, and A. Migus, Phys. Rev. Lett. **60**, 565 (1988).
[32]Y. Gontier and M. J. Trahin, J. Phys. B **13**, 4383 (1980).
[33]I. Ya. Berson, Izv. Akad. Nauk SSSR, Ser. Fiz. **45**, 2289 (1981) [Bull. Acad. Sci. USSR **45**, No. 11, 41 (1981)].
[34]S. P. Goreslavskiĭ, N. B. Delone, and V. P. Kraĭnov, Zh. Eksp. Teor. Fiz. **82**, 1789 (1982) [Sov. Phys. JETP **55**, 1032 (1982)].
[35]W. Gordon, Ann. Phys. (Leipzig) **2**, 1031 (1929).
[36]L. D. Landau and E. M. Lifshits, Quantum Mechanics, 3rd Ed., Pergamon Press, Oxford, 1977 [Russ. original, Nauka, M., 1974].
[37]N. B. Delone, S. P. Goreslavsky (Goreslavskiĭ), and V. P. Krainov, J. Phys. B **15**, L421 (1982).
[38]N. B. Delone, S. P. Goreslavsky (Goreslavskiĭ), and V. P. Krainov, J. Phys. B **16**, 2369 (1983).
[39]N. B. Delone, S. P. Goreslavsky (Goreslavskiĭ), and V. P. Krainov, J. Phys. B **22**, (1989).
[40]M. Trippenbach, K. Rzazewski, M. Fedorov, and A. Kazakov, J. Phys. B **22**, 1193 (1989).
[41]F. Fabre, G. Petite, P. Agostini, and H. Clement, J. Phys. B **15**, 1353 (1982).
[42]L. V. Keldysh, Zh. Eksp. Teor. Fiz. **45**, 1945 (1964) [Sov. Phys. JETP **20**, 1307 (1965)].
[43]A. I. Nikishov and V. I. Ritus, Zh. Eksp. Teor. Fiz. **52**, 223 (1967) [Sov. Phys. JETP **25**, 145 (1967)].
[44]A. M. Perelomov and V. S. Popov, Zh. Eksp. Teor. Fiz. **52**, 514 (1964) [Sov. Phys. JETP **25**, 336 (1967)].
[45]I. Berson, J. Phys. B **8**, 3078 (1975).
[46]N. L. Manakov and L. P. Rapoport, Zh. Eksp. Teor. Fiz. **69**, 842 (1975) [Sov. Phys. JETP **42**, 430 (1975)].
[47]H. Reiss, J. Opt. Soc. Am. B **4**, 1429 (1987).
[48]W. Becker, R. R. Schlicher, M. O. Scully, and K. Wodkiewicz, J. Opt. Soc. Am. B **4**, 743 (1987).
[49]Z. Deng and J. Eberly, Phys. Rev. Lett. **53**, 1810 (1984); J. Opt. Soc. Am. B **2**, 486 (1985).
[50]N. B. Delone, V. P. Krainov, and B. A. Zon, Zh. Eksp. Teor. Fiz. **75**, 445 (1978) [Sov. Phys. JETP **48**, 223 (1978)].
[51]A. M. Movsesyan and M. V. Fedorov, Zh. Eksp. Teor. Fiz. **94**, No. 3, 51 (1988) [Sov. Phys. JETP **67**, 462 (1988)]. M. V. Fedorov and A. M. Movsesian (Movsesyan), J. Opt. Soc. Am. B **5**, 850 (1988).
[52]K. Rzazewski and R. Grobe, Phys. Rev. Lett. **54**, 1729 (1985); Phys. Rev. A **33**, 1855 (1986).
[53]P. H. Bucksbaum, R. R. Freeman, M. Bashkansky, and T. J. McIlrath, J. Opt. Soc. Am. B **4**, 760 (1987).
[54]M. Levenstein, J. Mostovski, and M. Trippenbach, J. Phys. B **18**, 461 (1985).
[55]M. Trippenbach, J. Opt. Soc. Am. B **4**, 1429 (1987).
[56]A. Dolcic, Phys. Rev. A. **35**, 1673 (1987).
[57]J. Javanainen and J. H. Eberly, J. Phys. B **21**, L93 (1988).
[58]M. V. Fedorov, Zh. Eksp. Teor. Fiz. **52**, 1434 (1967) [Sov. Phys. JETP **25**, 952 (1967)].
[59]A. V. Gaponov and M. A. Miller, Zh. Eksp. Teor. Fiz. **34**, 242 (1958) [Sov. Phys. JETP **7**, 168 (1958)]; Zh. Eksp. Teor. Fiz. **34**, 751 (1958) [Sov. Phys. JETP 7, 515 (1958)].
[60]W. Xiong, F. Yergeau, S. Chin, and P. Lavigne, J. Phys. B **21**, L159 (1988).
[61]A. A. Radtsig and B. M. Smirnov, Reference Data on Atoms, Molecules, and Ions, Springer Verlag, Berlin, 1985. [Russ. original Énergoizdat, M., 1980 and 1986.]
[62]P. Kruit, J. Kimman, and M. van der Wiel, J. Phys. B **14**, L507 (1981).
[63]S. P. Goreslavskiĭ, N. B. Narozhnyĭ, and V. P. Yakovlev, Pis'ma Zh. Eksp. Teor. Fiz. **46**, 173 (1987) [JETP Lett. **46**, 219 (1987)].
[64]H. G. Muller, A. Tip, and M. van der Wiel, J. Phys. B **16**, L679 (1983).
[65]T. S. Luk, T. Graber, H. Jara, U. Johann, R. Boyer, and C. K. Rhodes, J. Opt. Soc. Am. B **4**, 847 (1987).
[66]J. Javanainen, J. H. Eberly, and Q. Su, Phys. Rev. A **38**, 3430 (1988). J. Eberli, J. Javanainen, and Q. Su, Kvant. Elektron. **15**, 1157 (1988) [Sov. J. Quantum Electron. **18**, 738 (1988)].
[67]I. Bondar', A. Gomonay, N. Delone, and V. Suran, J. Phys. B **17**, 2049 (1984). I. I. Bondar' and V. V. Suran, Opt. Spektrosk. **61**, 24 (1986) [Opt. Spectrosc. **61**, 15 (1986)]. D. Sh. Akramova, D. T. Alimov, N. B. Delone *et al.*, Izv. Akad. Nauk SSSR, Ser. Fiz. **45**, 1459 (1981) [Bull. Acad. Sci. USSR **45**, No. 8, 88 (1981)]. D. T. Alimov, A. N. Bel'kovskiĭ, V. K. Medvedeva, and M. A. Turnov, Zh. Prikl. Spektrosk. **44**, 211 (1986) [J. Appl. Spectrosc. **44**, 137 (1986)].
[68]A. McCown, M. Ediger, and J. Eden, Phys. Rev. A **26**, 3318 (1982) E. McGuire, Phys. Rev. A **24**, 835 (1981).
[69]G. Bethe and E. Salpeter, Quantum Mechanics of One and Two Electron Atoms, Springer-Verlag, Berlin, 1958 [Russ. transl., Fizmatgiz, M., 1960].
[70]V. P. Krainov and Z. G. Melikishvili, Opt. Spektrosk. **65**, 984 (1988) [Opt. Spectrosc. **65**, (1988)].
[71]D. T. Alimov, F. A. Il'kov, V. P. Krainov, and Z. G. Melikhishvili, in: *Elementary Processes in a Laser Radiation Field* (in Russian), Sovet Spektrosk. Akad. Nauk SSSR, M., 1987.
[72]I. Bondar (Bondar'), N. Delone, M. Dudich, and V. Suran, J. Phys. B **21**, 2763 (1988).
[73]S. Chin, D. Feldmann, J. Krautwald, and K. Welge, J. Phys. B **14**, 2353 (1981).
[74]A. I. Andryushin, A. E. Kazakov, and M. V. Fedorov, in: *Nonlinear Processes in Two Electron Atoms* (in Russian), Sovet Spektrosk. Akad. Nauk SSSR, M., 1984, p. 159; Zh. Eksp. Teor. Fiz. **82**, 91 (1982) [Sov. Phys. JETP **55**, 53 (1982)]; Zh. Eksp. Teor. Fiz. **88**, 1153 (1985) [Sov. Phys. JETP **61**, 678 (1985)].
[75]P. Lambropoulos and P. Zoller, in: *Multiphoton Ionization of Atoms* (Eds.) S. Chin and P. Lambropoulos, Academic Press, Toronto, 1984, p. 189.
[76]P. Gangopadhyay, X. Tang, P. Lambropoulos, and R. Shakeshaft, Phys. Rev. A. **34**, 2998 (1986).
[77]A. I. Andryushin and A. E. Kazakov, J. Phys. B **18**, 1501 (1985).
[78]K. Rzazewski and J. H. Eberly, Phys. Rev. A **27**, 2026 (1982).
[79]Yu. I. Heller and A. K. Popov, Phys. Lett. A **56**, 453 (1976).
[80]A. D. Gazazyan and R. G. Unanyan, Zh. Eksp. Teor. Fiz. **93**, 1590 (1987) [Sov. Phys. JETP **66**, 909 (1987)].
[81]S. A. Kotochigova, Zh. Eksp. Teor. Fiz. **94**, 104 (1988) [Sov. Phys. JETP **67**, 706 (1988)].
[82]I. I. Bondar' and V. V. Suran, in: *Elementary Processes in a Laser Radiation Field* (in Russian), Sovet Spektrosk. Akad. Nauk SSSR, M., 1987.
[83]D. Feldman, G. Otto, D. Petring, and K. Welge, J. Phys. B **19**, L144 (1986).
[84]S. Pratt, P. Dehmer, and J. Dehmer, Phys. Rev. A **35**, 3793 (1987).
[85]S. A. Kotochigova, in: *Nonlinear Spectroscopy of Atoms and Diatomic Molecules* [in Russian], Sovet Spektrosk. Akad. Nauk SSSR, M., 1988, p. 17.
[86]M. Aymar, Phys. Rep. **110**, 165 (1984).
[87]D. R. Alimov, I. I. Bondar', and F. A. Il'kov, Izv. Akad. Nauk SSSR, Ser. Fiz. **52**, 1124 (1988) [Bull. Acad. Sci. USSR **52**, No. 6, 72 (1988)].
[88]Z. G. Melikishvili, in: *Ionization Processes in Exited Atoms*, Abstracts of Conf. Reports (in Russian), Izd. Leningrad Univ., Leningrad, 1988, p. 56.
[89]D. T. Alimov, M. Yu. Ivanov, and F. A. Il'kov, in: Nonlinear Spectroscopy of Atoms and Diatomic Molecules (in Russian), Sovet Spektrosk. Akad. Nauk SSSR, M., 1988, p. 4.
[90]G. Leuchs and H. Walter, in: S. L. Chin and P. Lambropoulos (Eds.), *Multiphoton Ionization of Atoms*, Academic Press, N. Y., 1984, p. 109.
[91]O. Mullins, J. Hunter, J. Keller, and R. Berry, Phys. Rev. Lett. **54**, 410 (1985); Phys. Rev. A **31**, 3059 (1985); Phys. Rev. A **33**, 3138 (1986).
[92]A. Zangwill, J. Chem. Phys. **78**, 5926 (1983).
[93]S. V. Vlasov, B. A. Zon, I. Yu. Krivskiĭ, E. Yu. Remeta, and O. V. Farberovich, Perturbation Theory in Atomic Calculations [in Russian], Sovet Spektrosk. Akad. Nauk SSSR, M., 1985, p. 166.
[94]G. Wendin, L, Jonsson, and A. L'Huillier, J. Opt. Soc. Am. B **4**, 833 (1987).
[95]A. L'Huillier and G. Wendin, Phys. Rev. A **36**, 4747 (1987).
[96]A. L'Huillier and G. Wendin, Phys. Rev. A **36**, 5632 (1987).
[97]M. V. Ammosov, N. B. Delone, M. Yu. Ivanov, and V. P. Krainov, in: *Energy Levels and Transition Probabilities in Atoms and Ions* (in Russian), Sovet Spektrosk. Akad. Nauk SSSR, M., 1987, p. 5.
[98]P. Lambropoulos, Commun. Atom. Mol. Phys. **20**, 199 (1987).
[99]K. Boyer and C. Rhodes, Phys. Rev. Lett. **54**, 1490 (1985).
[100]K. Szöke and C. Rhodes, Phys. Rev. Lett. **56**, 720 (1986).
[101]M. Yu. Kuchiev, Pis'ma Zh. Eksp. Teor. Fiz. **45**, 319 (1986) [JETP Lett. **45**, 404 (1986)].
[102]I. D. Beigman and B. N. Chichkov, Pis'ma Zh. Eksp. Teor. Fiz. **46**, 314 (1987) [JETP Lett. **46**, 395 (1987)].
[103]H. Egger, U. Johann, T. Luk, and C. Rhodes, J. Opt. Soc. Am. B **3**, 901 (1986).
[104]S. Geltman, Phys. Rev. Lett. **54**, 1909 (1985).

[105]M. Crance, J. Phys. B **17**, 355, 635, 3503, 4333 (1984); **18**, L155 (1985).
[106]N. B. Delone, B. A. Zon, and V. P. Krainov, Izv. Akad. Nauk SSSR, Ser. Fiz. **50**, 773 (1986) [Bull. Acad. Sci. USSR **50**, No. 4, 132 (1986)].
[107]X. Mu, T. Aberg, A. Blomberg, and B. Grageman, Phys. Rev. Lett. **56**, 1909 (1986).
[108]I. A. Voĭtsekhovskiĭ and É. S. Parilis, Preprint Inst. Electron. Acad. Sci. Uzbek SSR No. 4 (In Russian), Tashkent, 1987.
[109]I. I. Bondar', M. I. Dudich, and V. V. Suran, Zh. Eksp. Teor. Fiz. **90**, 1952 (1986) [Sov. Phys. JETP **63**, 1142 (1986)].
[110]G. Petite and P. Agostini, J. Phys. (Paris) **47**, 795 (1986); Phys. Rev. A. **32**, 3800 (1985).
[111]U. Eichmann, T. Zhu, and T. Gallagher, J. Phys. B **20**, 4461 (1987).
[112]L. DiMauro, D. Kim, M. Courtkey, and M. Anselment, Phys. Rev. A **38**, 2338 (1988).
[113]N. Delone, V. Suran, and B. Zon, in: S. L. Chin and P. Lambropoulos [Eds.], Multiphoton Ionization of Atoms, Academic Press, N. Y., 1984, p. 235.
[114]P. Agostini and G. Petite, J. Phys. B **17**, L811 (1984).
[115]A. L'Huillier, L. Lompre, G. Mainfray, and C. Manus, J. Phys. B **16**, 1363 (1983).
[116]A. L'Huillier, L. Lompre, G. Mainfray, and C. Manus, Phys. Rev. A **27**, 2503 (1983).
[117]L. Lompre, A. L'Huillier, G. Mainfray, and C. Manus, J. Opt. Soc. Am. **2**, 1906 (1985).
[118]M. D. Perry, A. Szöke, O. L. Landen, and E. M. Campbell, Phys. Rev. Lett. **60**, 1270 (1988).
[119]S. Chin, K. He, and F. Yergeau, J. Opt. Soc. Am. B **1**, 505 (1984).
[120]U. Johann, T. Luk, H. Egger, and C. Rhodes, Phys. Rev. A **34**, 1084 (1986).
[121]T. S. Luk, U. Johann, H. Jara, I. A. McIntyre, A. McPherson, A. P. Schwarzenbach, K. Boyer, and C. K. Rhodes, SPIE **664**, 223.
[122]S. Chin, F. Yergeau, and P. Lavigne, Phys. Rev. B **18**, L213 (1985).
[123]S. Chin, W. Kloug, and P. Lavigne, J. Opt. Soc. Am. **4**, 853 (1987).
[124]M. V. Ammosov, N. B. Delone, and V. P. Krainov, Zh. Eksp. Teor. Fiz. **91**, 2008 (1986) [Sov. Phys. JETP **64**, 1191 (1986)].
[125]A. McPherson, G. Gibson, H. Jara, U. Johann, T. Luk, L. McIntyre, K. Boyer, and C. Rhodes, J. Opt. Soc. Am. B **4**, 545 (1987).
[126]M. Ferray, A. L'Huillier, X. Li, L. Lompre, G. Mainfray, and C. Manus, J. Phys. B **21**, L31 (1988).
[127]B. Shore and P. Knight, J. Phys. B **20**, 413 (1987).
[128]J. H. Eberly, Preprint Univ. Rochester, 1988.
[129]*Atomic and Molecular Processes in Short Intense Laser Pulses*, NATO Adv. Stud. Inst. Ser. B **171**, 1988.
[130]J. Zhang, H. Zhou, Q. Li, J. Yang, L. Zhao, and Y. Nie, J. Phys. B **21**, 589 (1988).
[131]K. Boyer, H. Egger, T. Luk, H. Pummer, C. Rhodes, J. Opt. Soc. Am. B **1**, 3 (1984).

Translated by A. Zaslavsky